REPORT ON

DETAILED ELECTRICAL GEOPHYSICAL SURVEYS

MT. TYNDALL AREA, NEAR QUEENSTOWN, TASMANIA

ON BEHALF OF

THE MOUNT LYELL MINING AND RAILWAY COMPANY LTD.

000

324002

PRIVATE AND CONFIDENTIAL

REPORT ON
DETAILED ELECTRICAL GEOPHYSICAL SURVEYS
MT. TYNDALL AREA, NEAR QUEENSTOWN, TASMANIA
ON BEHALF OF
THE MOUNT LYELL MINING AND RAILWAY COMPANY LTD.

BY

A.W. HOWLAND-ROSE
MSc,DIC,AMAusIMM,FGS.
GEOPHYSICIST

SYDNEY, N.S.W.

DECEMBER 1973 -
MARCH, 1974

TAS - 018C

CONTENTS

VI - Table of Stations and readings

Appendix 'IP'

Appendix 'T'

Appendix 'MIP'

Appendix 'IPR-8'

Plate 1 - Three Array Log

Plate 2 - Schlumberger Electrical Sounding

Plate 3 - Pole-Dipole and Three Array Detail Data Profiles

Plate 4 - Gradient Array Detail - West Grid Data Profiles

Plate 5 - Gradient Array Detail - East Grid Data Profiles

Plate 6 - Turam Electromagnetic Survey Data Profiles

REPORT ON

DETAILED ELECTRICAL GEOPHYSICAL SURVEYS

MT. TYNDALL AREA, NEAR QUEENSTOWN, TASMANIA

ON BEHALF OF

THE MOUNT LYELL MINING AND RAILWAY COMPANY LTD.

INTRODUCTION

At the request of Mr. K. Reid, Chief Geologist, for the Mount Lyell Mining and Railway Company Ltd., Scintrex Pty. Ltd. executed various detailed electrical geophysical surveys in the Mt. Tyndall area. In all, about 17 production days were involved.

These surveys wereunder the immediate direction of Mr. B. Ekstrom, with an additional operator being used on some surveys. The logistical support and field assistants were provided by the Mount Lyell Mining and Railway Company Ltd. Mr. A.W. Howland-Rose who provided technical supervision, made two trips to the area during the course of the surveys.

The geological supervision and direction was undertaken by Mr. K. Wells, Senior Exploration Geologist for the Mount Lyell Mining and Railway Company Ltd.

Appendices 'IP', 'T', 'MIP' and 'IPR-8' describe the various methods and equipment employed.

SCINTREX PTY. LTD.
Formerly
SEIGEL ASSOCIATES AUSTRALASIA PTY. LTD.
GEOPHYSICAL CONSULTANTS AND CONTRACTORS

SUMMARY

Five separate projects at Mt. Tyndall are discussed in detail in this report. The down hole work at Mt. Tyndall did not show the non-economic copper mineralisation to have a unique signature against the disseminated pyritic halo, while the Electromagnetic survey did not reveal anomalies considered of major significance. Gradient detail over a number of the geologically significant anomalies located in the 1967/8 McPhar surveys have enhanced their interest, while others shows less significant responses.

1031 WELLINGTON STREET, WEST PERTH, W.A. 6005
TELEPHONE 21 6934. TELEGRAMS "SCINTREX" PERTH

6 TRAMORE PLACE, KILLARNEY HEIGHTS, N.S.W. 2087
TELEPHONE 451 5367. TELEGRAMS "SCINTREX" SYDNEY

I - THREE ARRAY LOG, HFZ1

DISCUSSION OF RESULTS

This hole was drilled on line 63 to investigate an induced polarization zone considered to be of significance and described in detail on page 30 of Report TAS-016. The work was carried out by B. Ekstrom on the 5th December, 1973.

The array consisted of a five feet three array log. A diagrammatic representation of the current paths and equipotential field is shown in the figure, and a to-scale representation is shown on Plate 1.

The data profiles of the log are shown in Plate 1 at the down hole scale of 1 inch = 25 feet, while the chargeability is shown at the scale of 1 inch = 20 milliseconds and the resistivity on a two inch log cycle, expressed in ohm-metres. Also displayed at suitable scales are the pyrite and copper percentages recorded in the hole.

The array used, effectively samples for a distance around the hole of about five feet. When allowance is made for geometric effects, it can be quite clearly seen that the more conductive zones are due to the presence of pyrite. However, absolute levels of resistivity recorded in the

EQUIPOTENTIAL DIAGRAM

DOWN HOLE THREE ARRAY LOGGER

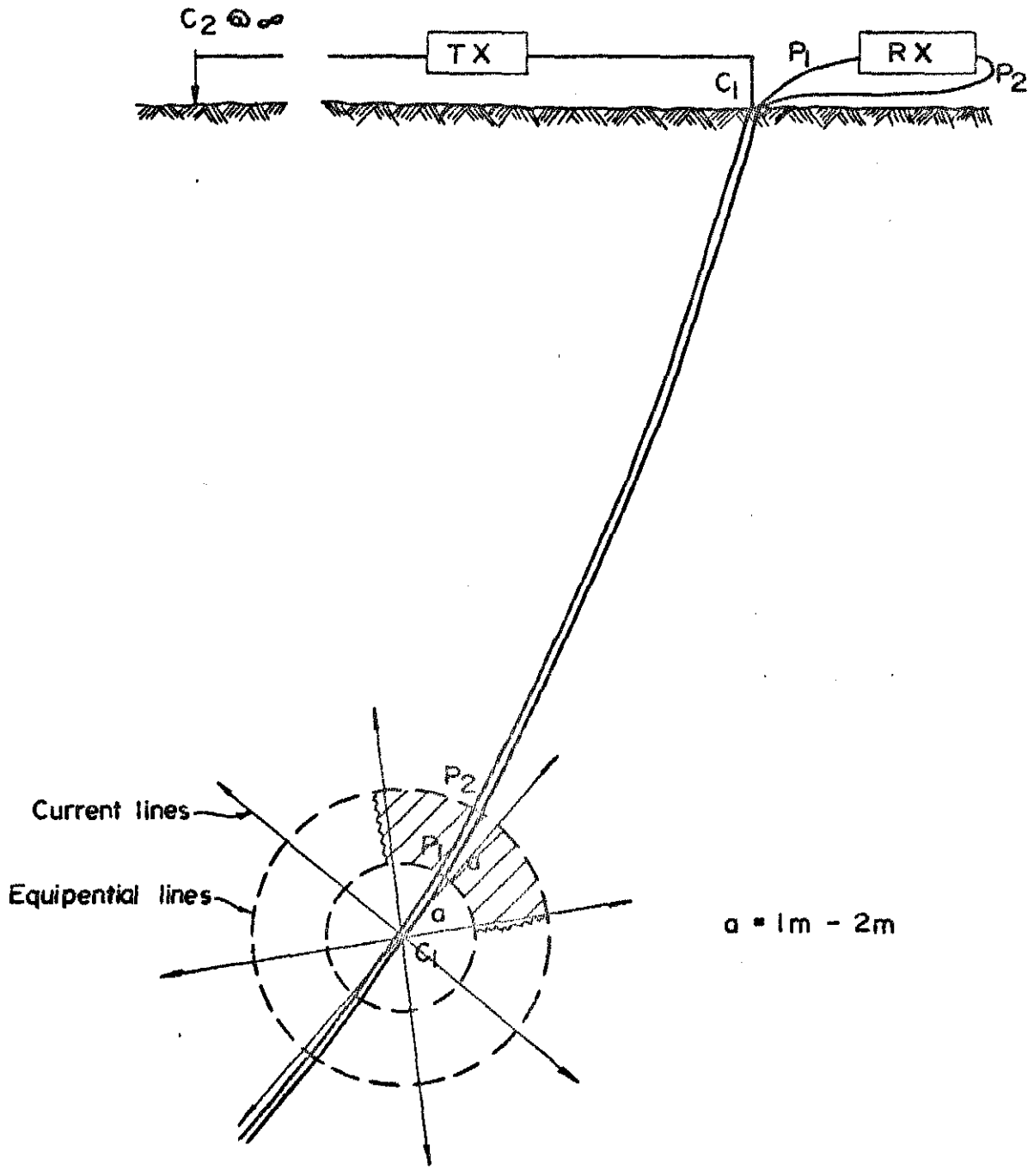

conductive zone are never less than 50 ohm-metres, which is not considered to be conductive. The conductivity is certainly not sufficient to be detected by an electromagnetic method.

As would be expected, the chargeability recorded, mirrors the total sulphide content, the relationship being 1% sulphide to about 10 to 20 milliseconds which is within the range of those normally observed.

CONCLUSIONS

1 - The induced polarization response located on the surface can be clearly identified in the diamond drill hole.

2 - The bulk conductivity ranges between 1000 ohm-metres and 50 ohm-metres. The lowest apparent resistivities reflect those sections of the hole having in excess of 1% pyrite in most cases.

3 - A similar relationship between chargeability and total sulphides is apparent, but as the chargeability is proportional to the total surface area of the sulphides, its absolute level will depend on grain size as well as volume.

4 - The copper mineralisation, as would be expected from the geochemical log, has no distinct signature. Both the chargeability and resistivity reflect the total volume of sulphides, adjusted for effective grain size.

5 - The log was carried out using an IPR-7 single channel receiver. Thus, any differences in decay form would be difficult to detect. However, significant changes in L/M ratio have been recorded down hole. The two induced polarization zones from 400 to 445 and from 465 to 470 are inferred to be more finely disseminated than that centred at 325. The dissemination between, is inferred to be much coarser, for example from 370 to 385.

RECOMMENDATIONS

1 - Any further logs should be run with the IPR-8 using all six slices (See Appendix 'IPR-8'). In this way, significant changes in decay curve can be identified. Should significant changes occur in mineralised sections of significance, the MIP technique may be able to identify these from ground surveys on the surface, thus enabling a better selection of targets to be made.

2 - No applied potential or applied chargeability surveys down the hole are recommended as the conductive sections

are not associated with the copper mineralisation as such, but with the pyrite zone.

II - SCHLUMBERGER ELECTRICAL SOUNDING

CENTRED ON LINE 56 AT 00

INTRODUCTION

This electrical sounding, to obtain further information as to the depth of glacial moraine on the road near line 53 on the Tyndall grid, was carried out by B. Ekstrom on the 3rd March, 1974,

An electrical sounding was carried out over the same moraine at a different locality in the 72/73 field season and is shown in Plate 5 of report TAS-016.

DISCUSSION

Plate 2 displays the results of the sounding using a 5 inch log cycle to display the apparent resistivity in ohm-metres on the vertical scale, while the spacing is shown on the horizontal scale in feet. The apparent chargeabilities shown are at a scale of 1 inch = 10 millivolts/volt, while the (Ma - M1) is shown in millivolts/volt also on a log scale.

A diagrammatic representation of the interpretation is shown on Plate 3. A layer of about 17 to 18 feet in thickness and having a resistivity of 3600 ohm-metres is

interpreted to lie near surface. The chargeability of this zone is estimated to be of the order of 7 millivolts/volt. A second contrast at about 200 feet is inferred, where again it is resistive. The centre section from 17 feet to 200 feet has an apparent resistivity of 100 to 200 ohm-metres.

An increase in chargeability from 7 millivolts/volt to 140 millivolts/volt is interpreted at a depth of the order of 30 feet.

CONCLUSIONS

The form of the sounding is similar to that observed in the 72/73 survey, but the depths are different. If the glacial moraine is in fact resistive relative to the underlying unit, then the estimated depth is of the order of 17 feet. However, if the underlying rocks are resistive and the glacial moraine is conductive (the usual case) then the moraine depth is of the order of 200 feet.

As the gradient resistivity data shows the rock unit below to be conductive, the former solution is favoured, giving a depth to the bedrock of about 17 feet.

III - DETAILED POLE-DIPOLE AND THREE ARRAY

INTRODUCTION

The work was carried out on four production days between 28th February and 2nd March, 1974.

DISCUSSION

Close coupled array detail was surveyed over line 52 and 53 between 0 and 28E. This data is displayed in Plate 3 at a horizontal scale of 1 inch = 200 feet and vertical scales of 1 inch = 10 millivolts/volt for the induced polarization response and a two inch log scale was used for the resistivity which was expressed in ohm-metres.

The chargeability was recorded in terms of millivolts/volt on the Scintrex IPR-8 multi-channel receiver, the details of which are given in Appendix 'IPR-8'. Three separate channels, M_1, M_3 and M_5 were recorded, of which only M_3 has been plotted. The relationship between millivolts/volt and milliseconds is also given in detail in Appendix 'IPR-8', but 1 millisecond is approximately equal to $1\frac{1}{2}$ millivolts/volt.

Two electrode geometries were employed, potential diagrams of which are shown, to scale, on Plate 3.

The Pole-Dipole Survey on Line 52 employed a spacing of 200 feet at n=1 and n=2. The line was surveyed between 2E and 27E at both spacings. Two sections of the line between 2E/8E and 20E/28E were also surveyed using a three array geometry with spacings of 50 feet and 100 feet. The former covered anomalies 59 and 60 and 61, and the latter 61 and 59 respectively, as described in Report TAS-016 on page 24.

Anomaly 59 The gradient array survey positioned this response at 2450E, but the western flank of the anomaly was electromagnetically coupled. The pole-dipole array shows higher than background values between 16E and 24E. Although the response decreases with increasing electrode spacings, the absolute levels of 15 millivolts/volt (10 milliseconds) are slightly less than the magnitude of the gradient response. The local background is about 10 millivolts/volt ($6\frac{1}{2}$ milliseconds) which is the same as for the gradient array. The three array data shows a significant response of 19 millivolts/volt (13 milliseconds) centred at 21E from a source whose maximum depth is less than 50 feet. The smaller spread three array shows a distinct increase in resistivity with increasing spacing, inferring a local, more conductive layer some 70 feet deep, having a resistivity of 1000 ohm-metres or so, assuming a two layer case. However, the gradient array gives much

lower resistivity values between 18E and 24E, showing that at depth, between these co-ordinates, the zone is much more conductive. The gradient array is much less affected by near surface inhomogeneities in the resistivity, giving it the ability to "see" through them. The zone of much increased conductivity must be deeper than the effective penetration of the greatest spacing used, i.e. deeper than 300 feet or so.

Anomaly 60 The gradient anomaly of 7 milliseconds at 18E is confirmed by the pole-dipole data. However, the maximum response is less on the pole-dipole data than the gradient, inferring an increase in chargeable material to depth. The depth is assessed to be between 100 and 200 feet.

Anomaly 61 The sharp, well defined, narrow gradient response of 6 milliseconds above background at 6.5E was detailed with a 50 feet and 100 feet three array, between 2E and 8E, and is confirmed by this array. The maximum depth is assessed to be less than 50 feet and the width perhaps 20 feet or so. The resolving power of the gradient array is dramatically shown in that there is only minor response at a=100 feet and no response with the pole-dipole array.

A second narrow zone only seen on the a=50 feet three array profile was detailed for a source at 4.5E.

Although the L/M ratio on the gradient array showed a marked depression over the above zone, indicating a long time constant for the decay of the induced polarization effect, M_5 is slightly more than M_1. These two factors infer that the near surface mineralisation is fairly disseminated within a resistive source, but to depth the grain size increases and the source is less resistive than the enclosing rocks.

Line 53 Anomalies 62 and 63 described in Report TAS-016 on page 25. The pole-dipole and three array detail was run over both zones, while the pole-dipole was used between 1E and 28.5E.

Anomaly 63 This zone is situated on the gradient array at about 5.5E. The broad low amplitude induced polarization response on the pole-dipole data at about 7E may be the up dip surface manifestation of this response, which has an inferred west dip. However, the three array 50 feet spacing shows a low amplitude but definite response from a source at about 5E to 5.75E, coincident with the gradient array, which is not seen on the pole-dipole array. It therefore appears that the gradient array has resolved narrow zones not seen

with the larger spaced pole-dipole. The 50 feet spaced three array also infers the zone to be conductive with respect to the enclosing rocks. The gradient data shows this, but the absolute resistivities are much higher, indicating an increase in resistivity with depth.

Anomaly 62 Neither the pole-dipole or three array was run sufficiently far east to completely cover the zone of interest. However, two anomalous induced polarization responses from narrow shallow sources are seen at 23.5E and 25.5E. The pole-dipole data shows slightly higher backgrounds were recorded east of 20E coincident with an increase in resistivity. This is in marked contrast to the results recorded with gradient array.

In view of the apparent efficiency of the gradient array in resolving narrow bodies described above, it is considered likely that the low resistivity and high chargeability come from a zone at a depth greater than the 250 to 300 feet depth penetration obtained with the pole-dipole. The interest of this zone remains.

CONCLUSIONS AND RECOMMENDATIONS

1 - The gradient data certainly appears superior to large spaced pole-dipole (and therefore dipole-dipole) in resolving narrow chargeable zones. Only at 50 feet

spacings were comparable responses obtained. Rarely did the pole-dipole data give any significant response.

2 - As all zones have now been well defined (except that at 2.6E/Line 52) as to position and maximum depth, drilling is recommended if these have potential economic interest as gauged from ancillary data such as geochemistry.

IV - GRADIENT ARRAY EIP DETAIL

ON EAST AND WEST GRIDS, MT. TYNDALL

INTRODUCTION

As a result of a study of McPhar 1967/68 surveys carried out over the East and West grids at Mt. Tyndall, summarised in Consultancy Report C-033 dated November, 1973, detailed surveys were executed over selected zones. These surveys were undertaken by Scintrex operator Mr. B. Ekstrom on 7 days between the 11th and 20th December, 1973.

DISCUSSION

The receiver employed to record the IP effect was the Scintrex IPR-7 and the units of chargeability used are milliseconds.

A - West Grid

The data is presented in Plate 4 at the horizontal scale of 1 inch = 200 feet with chargeability at the scale of 1 inch = 10 milliseconds and resistivity expressed in ohm-metres on a two inch log scale.

Two current dipoles were employed to cover the zone of interest as follows:

Electrodes	Dipole	Lines
20W and 30E on 26	5000 feet	24, 26, 28
18.5W and 1.5E on 26	2000 feet	26

A line by line description of the data is given below.

Line 28 The McPhar data is shown on drawing 5107-14 dated 22nd May, 1968. The section repeated in the present survey was between 17.5W and 19.5E.

The background apparent resistivity remains between 1000 and 3000 ohm-metres for the most part, with rapid fall-offs east of 18.5E and west of 17.5W. At about 11.5W a broad resistivity high, in excess of 20,000 ohm-metres, was defined with boundaries at about 13W and 10.5W. This represents a most resistive rock unit.

Between 14.5W and about 18E the chargeabilities recorded remain at about 30 milliseconds, with local highs at 7.5W and between 10E and 16E. This whole zone is anomalous and, as the absolute values of the resistivity within this zone are never less than 1000 ohm-metres, and often above 3000 ohm-metres, the source must either be disseminated graphite or disseminated sulphides. The L/M ratio is everywhere normal, ranging about 0.8 $\pm$0.1

Line 26 The original McPhar dipole-dipole data is displayed on drawing 5107-13. The resistivity recorded on this line shows a range in resistivity from just in excess of 3000 ohm-metres to about 100 ohm-metres.

Several quite distinct chargeability levels were recorded as follows:

18W - 8.5W	19 ± 3 milliseconds
8.5W - 4E	30 ± 3 milliseconds
4E - 10E	about 40 milliseconds
10E - 14.5E	about 18 milliseconds
14.5E - 22E	27 ± 3 milliseconds

The absolute levels of resistivity recorded, generally indicated either disseminated sulphide or graphite sources between 8W to 10E, or if 'massive', the mineralisation is inferred to be electrically discontinuous.

Within the highly chargeable horizons, a number of distinct local highs were recorded.

At 7.75W a narrow zone lies at an estimated maximum depth of 40 feet, and has an asymmetry which suggests an east dip.

A minor, but well defined reduction in apparent resistivity to about 800 ohm-metres from 1500 ohm-metres at 8W, infers weak conduction within the source.

Between 6E and 9E a very substantial induced polarization anomaly of just under 50 milliseconds is estimated to come within 100 feet of surface at 6.5E, having an east dip and a width of the order of 200 to 250 feet. Although there is a reduction in the apparent conductivity across this zone, to about 4000 ohm-metres against 1500 ohm-metres to the immediate east and west, the causative material is not considered to be overly conductive.

A high chargeability response at 4.5E is associated with a small but perhaps significant depression in the resistivity profile. The maximum depth is assessed to be about 60 feet.

A broad resistivity low at 19.5E, of about 120 ohm-metres from a background of 900 ohm-metres is coincident with a low amplitude reduction in induced polarization background from a high 30 milliseconds to 24 milliseconds. As the chargeability background remains high, weakly conductive sulphides (or graphite) is considered to be the source.

Line 24 The McPhar data is displayed on drawing 5107-12.

A broadly similar picture is presented on this line, with various distinct chargeability background levels as set out below. They correlate with those of the previous line (26) as shown.

Line 24		Line 26
16.5W - 12W	about 13 milliseconds	18W - 8.5W
12W - 0.5E	about 30 milliseconds	8.5W - 4E
0.5E - 6.5E	about 35 milliseconds	4E - 10E
6.5E - 10.5E	20 $\pm$ 4 milliseconds	10E - 14.5E
10.5E - 15.5E	about 34 milliseconds	14.5E - 18E
15.5E - 19.5E	9 milliseconds	- - - -

Within these backgrounds a number of distinct anomalies stand out. At 14.5W a 7 millisecond anomaly was recorded on a 12 millisecond background. There is a minor depression in the high resistivity of 10,000 ohm-metres and the source is therefore considered to be disseminated. The maximum depth is 130 feet. This is probably the correlative of a minor anomaly located at 12.5W on line 26.

A major anomaly of about 20 milliseconds superimposed on a background of 23 milliseconds to the east, was recorded at 4.0E. The maximum depth to the top of the body is assessed to be not greater than 80 feet at this point. The response shows no material resistivity contrast with

the adjacent background and remains at about 1000 ohm-metres. The source is therefore considered to be disseminated. This zone is undoubtedly the correlative of that seen on line 26 at 6.5E.

The small response at 4.5E described on line 26 has a definite more material correlative on this line at 0.75E where a sharp, narrow, steeply east dipping source is assessed to lie within 100 feet of surface. A broad resistivity low displaced slightly west may represent the up dip manifestation of this zone.

A single point high at 8.5E within a slightly more conductive host, has no correlative on line 26.

The broad chargeability high centred at about 16.75E on line 26 has an expression on this line at 13.5E. West of 15E the chargeability falls rapidly to a background of 9 milliseconds.

CONCLUSIONS

1 - Lines 26 and 24 show similar chargeability patterns, individual chargeability highs within the high background being able to be correlated with certainty. However, line 28, although it has the same very high

background chargeabilities as recorded on lines 24 and 26, does not show any detailed correlation.

2 - The very high chargeabilities detected from sources within 200 feet of the surface, and often within 50 feet of surface, in both the dipole-dipole and gradient array data, will mask responses beneath them. Both surveys therefore represent relatively near surface response. The depth to which gradient array is able to energise, remains undiminished however, and the resistivity data has effectively much greater penetration. However, in the present situation the resistivity is not considered to be diagnostic.

3 - For the most part the lines are considered to be anomalous over the entire length of line. The inferred percentage of pyrite or graphite over the entire length of line is 2% by volume. In these circumstances it is not possible to isolate individual chargeability peaks within the high background as being significant.

4 - The impression gained from an examination of the data, based on experience in the region, is that the majority of the responses will be found to come from graphite.

RECOMMENDATIONS

1 - It is not possible to pick out individual induced polarization responses for particular follow-up. The significance of each high will have to be established by methods other than electrical induced polarization. Should geological mapping and/or soil geochemistry not be feasible due to glacial cover, auger drilling may be required.

2 - In the future it may be possible to isolate zones of interest within the broad disseminated pyrite or graphite zones defined on lines 24, 26 and 28 by measuring the internal decay form which more massive mineralisation would have. It remains to be demonstrated that known copper zones have characteristic decay forms. Unfortunately this can only be researched when suitable frequency domain magnetic induced polarization equipment is available in Australia.

B - East Grid

The data is presented in Plate 5 at scales as per Plate 4.

Lines 28N to 40N Each individual line is described below.

Line 28N A 2000 feet current dipole with electrodes at

40W and 20W together with a 100 feet potential dipole was used to investigate line 28N between 23.5W and 33.5W. The background chargeability remains a normal 10 milliseconds with a depression to a low 3 milliseconds at 28.5W. This significant reduction in chargeability is coincident with a significant reduction in apparent resistivity to less than 400 ohm-metres compared with some 1300 ohm-metres to the immediate east and 8000 ohm-metres to the west. Conductive, non-chargeable clays or oxidation are suggested interpretations.

The McPhar data is displayed on plates 2679-29 (300 feet) 2679-30 (200 feet) and 5108-41 (100 feet). The importance of metal factor anomalies at this point is not confirmed.

Line 34 A current dipole of 2000 feet was placed between 9W and 29W to investigate this line between 25.5W and 15.5W. The 100 feet potential dipole recorded backgrounds of about 9 to 11 milliseconds with a minor single point chargeability high at 18.5W. A broad resistivity low was defined between 21.5W and 17.5W.

The McPhar data is displayed in plates 5108-46 (100 feet) 2679-36 (200 feet) and 2679-37 (300 feet). The portion of the anomaly at 20W on the dipole-dipole data, is clearly shown to lie vertically below 18.5W and as the anomaly is

of limited size, it is not considered of significance unless geochemistry or geology enhance its interest.

Line 38N This line, together with lines 40, was energised using a 6000 feet current dipole placed on line 40 at 50W and 10E. A potential dipole of 100 feet was used to investigate the resultant potential field.

The background chargeability recorded over the line ranges between 7 and 12 milliseconds while the apparent resistivities show variations from 3000 ohm-metres to in excess of 20,000 ohm-metres.

Two very well defined zones centred at 12.5W and 10.5W have sources of estimated widths of 140 feet and 80 feet respectively. The estimated maximum depths are 150 feet and 100 feet respectively, while the inferred dip is steep to the west. The source is considered to be disseminated, or if "massive", electrically discontinuous, as there is only a minimal reduction in the observed apparent resistivity.

An almost identical set of anomalies was recorded centred at 32W and 33.5W respectively. The dip of the sources appears to be vertical and the widths of the source, about 80 feet. The maximum depth is estimated less than 100 feet. The anomaly at 33.5W has associated 60%

reduction in apparent resistivity to 5000 ohm-metres. Although some increase in the conductivity within the source is indicated, the absolute levels of the apparent resistivity infer a disseminated source.

Between 34W and 39W the resistivity rises to 18,000 ohm-metres, while the chargeability is reduced to less than 2 milliseconds at 38W. A highly resistive, perhaps silicified unit is suggested as the source of these features.

West of 39W the chargeabilities rise rapidly to about 28 milliseconds to the end of the line at 47.5W. Over this zone the apparent resistivities are reduced to 4000 to 7000 ohm-metres from 18,000 ohm-metres to the east. A disseminated source is suggested for the chargeability, either graphite or pyrite. The contact at 39W is sharp, indicating a well defined contact between units of very different electrical properties, and abruptness in change also indicates the maximum depth to be less than 100 feet at the contact.

Line 40 The background resistivities and chargeabilities show the same range on this line as on line 38.

Within an anomalous zone between 9W and 4W, distinct chargeability highs of 25 and 12 milliseconds above

background were recorded centred at 6.7W and 5.0W respectively. Both sources are estimated to be in excess of 100 feet wide, and have maximum depths of less than 150 feet. The asymmetry of the profile infers a steep west dip. As with their correlatives at 12.5W and 10.5W on line 38, very weak conduction is suggested within the disseminated source.

A very slight rise in chargeability of some 4 or 5 milliseconds above background coincident with a 70% reduction in apparent resistivity to 2000 ohm-metres at 24.5W is thought to be the correlative of the substantial anomaly recorded at 33.5W on line 38N.

Between about 25W and 32W the resistivities rise to just over 10,000 ohm-metres. This probably is the correlative of the highly resistive zone between 34W and 39W on line 38N.

West of 34W chargeability rises from about 10 milliseconds to 18 milliseconds with two anomalies of some 6 and 10 milliseconds above background at 35W and 44.5W. However, no correlative to the very high chargeabilities west of 39W on line 38N were defined.

Zone A The data is shown in Plate 5 at a horizontal scale of 1 inch = 200 feet. The chargeability and resistivity

scales are as for the other detailed zones.

The original McPhar data is shown on drawings 5108/2, 5108/4, 5108/4A. 5018/5 and 5108/7

A 2000 feet gradient array was emplaced on line 6 + 00 at 10E and 10W to investigate lines 6 + 400N, 6 + 00 and 6 + 400S. In all three cases a 100 feet potential dipole was employed to investigate the resultant potential field.

All three lines surveyed show a very highly chargeable zone of 20 to 25 milliseconds above background as follows:

6 + 400N	2.5W - 5.5E
6 + 00	5.0W - 5.0E
6 + 400S	3.0E - ?

Within these zones local chargeability peaks or shoulders suggest interline correlation as follows:

6 + 400N	1.5W	0.5E
6 + 00	1.75W	0.5E
6 + 400S	3.25E	6E

The gradient array infers this zone to be due to a disseminated or electrically discontinuous source which in places comes within 50 feet or so of surface. Although there is a reduction

in resistivity over some sections, the absolute levels of 1000 ohm-metres preclude significant conduction.

The anomalies at 1.75W and 0.5E on line 6 + 00 are considered to have maximum depths of 60 to 80 feet as are those at 3.25E and 6E on line 6 + 400S. Initial investigation of this zone should be concentrated at these zones.

Zone C-3 The data profiles are presented on Plate 5 at the horizontal scale of 1 inch = 200 feet with vertical scales as for previously discussed detail.

The three lines, 22 + 200N, 22 + 00 and 22 + 200S, were surveyed using a 2000 feet current dipole with electrodes at 12W and 32W on line 22 + 00. The original McPhar data is shown on plates 5108-33/5.

Each line is described separately below.

Line 22 + 200S Two distinct and significant anomalies were defined by the gradient array. At 23W, a 20 millisecond response against the 10 millisecond background is interpreted to come from a source within 120 feet of surface. The width of the chargeable zone is considered to be just in excess of 100 feet and the asymmetry suggests a steep east dip. The absence of any material reduction in apparent chargeability

together with the absolute level of about 1000 ohm-metres suggests a disseminated source.

A second 20 millisecond response at 18.5W is interpreted to come from a disseminated source showing some weak conduction and having a width of about 80 feet and a maximum depth of about 70 feet.

Line 22 + 00 Both the anomalies above have correlatives on this line as follows:

22 + 00	22W	19.5W
22 + 200S	23W	18.5W

The response at 22W is less than half that of its correlative on line 22 + 200S, but still forms a significant anomaly. However, in this case, instead of there being no decrease in apparent resistivity there is an increase over the chargeable zone. The source is therefore either disseminated or, if massive, electrically discontinuous, and may in fact be silicified.

The substantial 15 millisecond response recorded at 19.5W is estimated to have a maximum depth of 50 to 60 feet, a width of the order of 50 feet and dips steeply to the east. There is a reduction in apparent resistivity, indicating

weak conduction within the source. However, the absolute level still suggests a disseminated source.

Line 22 + 200N The general form of both apparent resistivity and apparent chargeability are differenct on this line to those described on the lines to the immediate south. A 20 millisecond response was recorded between 26W and 20W with a slight peak at 20.5W. As the resistivities remain high, a disseminated graphite or pyrite source is suggested.

Zone B The usual vertical scales and horizontal scales are used to display the data for line 4 on Plate 5. A 2000 feet gradient was positioned with electrodes at 46E and 66E and a 100 feet potential dipole was employed to investigate the resultant potential field. The original data is shown in McPhar drawing 5108-1. The section of the line detailed runs between 49.5E and 60.5E.

Although both sets of data show the same general picture, the gradient data clearly demonstrates that the section west of 51.5E is entirely anomalous and no differentiation within this zone on a basis of chargeability is possible. A local induced polarization maximum was noted at 53E, just east of a sharp boundary between 20/25 millisecond chargeabilities to the east, and 5 milliseconds background to the west.

Although sharp changes in resistivity were noted at 50E, 52.5E and 55.25E, the entire section has resistivities in excess of 400 ohm-metres and therefore the source is considered to be disseminated in nature.

CONCLUSIONS AND RECOMMENDATIONS

1 - The detailed work carried out on lines 28N and 30N did not confirm the interest of the dipole-dipole anomalies located on these lines. Therefore no further work is recommended unless geological and/or geochemical data infers an economic potential in the area.

2 - The substantial induced polarization anomalies between 10W and 13W on line 38N, 31W and 34W on line 38N and between 4W and 8W on line 40N, are recommended for follow-up as targets of primary interest. Although some conduction within the host is suggested by a reduction in the recorded apparent resistivities, the sources are considered to be either disseminated pyrite or graphite (or if "massive", electrically discontinuous)

3 - The very highly chargeable zone west of 39W on line 38 is considered to be due to either disseminated graphitic or pyritic material. The absolute level of resistivity suggests a disseminated source, while the level of

chargeability suggests about 1% to 1½% sulphides (or graphite) throughout the entire section between 39W and 47W. Follow-up to ascertain if this zone is a pyritic halo should be undertaken.

4 - The minor anomalies at 35W and 44.5W on line 40 should be examined on the ground to ascertain their possible economic interest.

5 - On Zone A a broad chargeable zone from a disseminated graphitic or pyritic source was located. Four induced polarization highs at 6 + 00/1.75W, 6 + 00/0.5E, 6 + 400S/3.25E and 6 + 400S/6E were defined from sources within 60 to 80 feet of surface. These anomalies are recommended for further ground follow-up.

6 - With regard to the detail carried out over anomaly C the gradient array has enhanced interest in the area. It is significant that the pole-dipole, even at a = 100 did not resolve individual anomalies on either line 22 +00 or line 22 + 200S.

The two zones listed below are considered significant and are recommended for careful follow-up:

22W and 23W on lines 22 and 22 + 200S

19.5W and 18.5W on lines 22 and 22 + 200S

6 - On line 4, Zone B is revealed to be an undifferentiated zone of high chargeability west of about 51.5E. This is due to either disseminated graphite or pyrite. If the latter, it may represent a portion of the halo in which the copper deposits occur.

V - ELECTROMAGNETIC SURVEY OF LINES 54N TO 61N

INTRODUCTION

On four days between 6th and 9th January, 1974, two Scintrex operators under the direction of Mr. B. Ekstrom executed Turam Electromagnetic surveys on lines 54N to 61N, in an attempt to define electromagnetic conduction within a broad zone of high chargeability considered to be a possible pyrite halo around copper mineralisation.

DISCUSSION

The data profiles are presented in Plate 6 at the horizontal scale of 1 inch = 200 feet with vertical scales of 1 inch = 10^{o} phase shift and 1 inch = 20% field strength ratio.

Two energising loops were employed to survey the area, each of 3000 feet by 4000 feet. The leading edge of the most northerly of the two was at line 61/24E with the loop to the east, whilst the southern loop was situated to the south and the leading edge running grid north from 22E on 54N.

The energising frequency used as variously 400 Hz and 800 Hz as shown on Plate 6.

The only anomalies located on the grid area were in the southern quadrant and were generally not well defined.

The characteristics of these sources are given below.

Line	Station	Max. Depth	st	Definition
56N	3W	?	21 mhos	weak
55N	4.8W	200 feet	16 mhos	moderate
55N	2.5W	?	21 mhos	weak
54N	3.5W	?	21 mhos	weak

CONCLUSIONS AND RECOMMENDATIONS

Only in the event of these zones proving to be of possible economic interest due to their geologic setting or due to anomalous geochemistry, should further investigation by drilling be contemplated, as these zones are barely resolved from background, and lie within a zone of low apparent resistivities are recorded by the gradient array.

Respectfully submitted on behalf of:

SCINTREX PTY. LTD.

A.W. HOWLAND-ROSE, MSc,DIC,AMAusIMM,FGS.

GEOPHYSICIST

APPENDIX 'I.P.'

INTRODUCTION

For the benefit of those who are unfamiliar with the Induced Polarization method in general, or with the pulse-type method in particular, a few introductory remarks will be directed on the Induced Polarization, or overvoltage, phenomenon. Those who wish a fuller treatment of the subject are directed to Seigel (1962), which paper also includes an extensive list of references.

Induced Polarization in its broadest sense means a separation of charge to form an effective dipolar (polarised) distribution of electrical charges throughout a medium under the action of an applied electric field. When current is caused to pass across the interface between electrolyte and a metallic conducting body, double layers of charge are built up at the interface, in the phenomenon known to electrochemists as "overvoltage". This is the phenomenon which can be utilised for the detection of metallic conducting, rock-forming, minerals such as most sulphides, arsenides, a few oxides and, unfortunately, graphite. In addition, effective dipolar charge distribution occurs to some extent in all rocks, due to ion-sorting in the fine capillaries in which the current is passing.

Induced Polarization responses may therefore arise from metallic or non-metallic agencies. Fortunately, the latter generally falls within fairly low and narrow limits for almost all rock types, although there is still no reliable criterion for differentiating overvoltage responses from graphite and metallic sulphides, or for distinguishing between the responses of one type of sulphide and another. Despite these limitations the Induced Polarization method has amply demonstrated its value in mineral exploration since its initial development as a useful exploration tool in 1948 (ed. Wait, 1959).

DESCRIPTION OF METHOD AND EQUIPMENT

For the present programme the pulse or time domain system was employed, using a Scintrex Induced Polarization unit. The standard current-wave form with the unit is two seconds on-time and two seconds off-time. (see Figure 1). This unit features the Newmont type self-triggered receiver which operates remote from the current transmitting equipment. Three fundamental quantities are measured with this unit - the chargeability of 'M' measurement, the 'L' measurement and the resistivity.

The receiver integrates the area under the decay curve during the time interval from 0.45 seconds to 1.1. seconds

MEASUREMENTS TAKEN

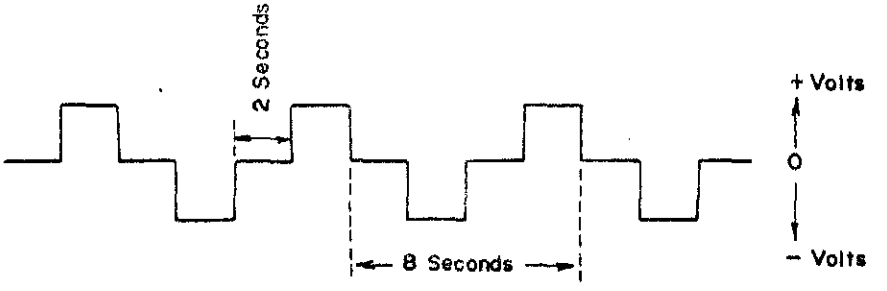

Energising frequency is a square wave having a frequency of 0·125 cps.

FIELD MEASUREMENTS MADE

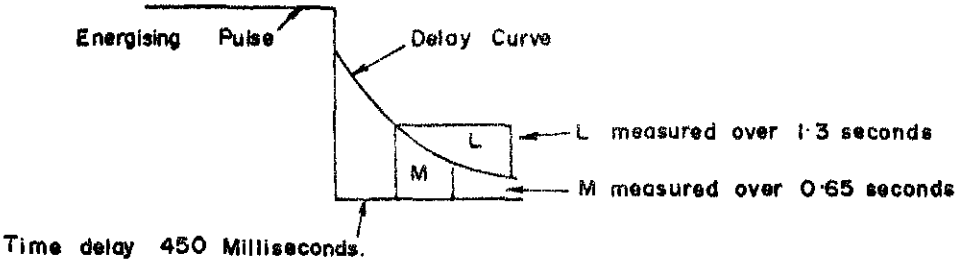

Fig. 1

after termination of the primary current pulse. This integral normalised with respect to its corresponding primary voltage is the chargeability or 'M' measurement, that is, the fundamental Induced Polarization characteristic. It is in units of milliseconds. The Induced Polarization phenomena is dependent on the existence of electronically conducting material within the matrix of ionically conducting material. The chargeability is therefore a measure of the presence of electronically conducting material within the ground being tested.

The second quantity measured is the area over the transient decay curve between 0.45 seconds and 1.75 seconds of the current off-time. This measurement is designated the 'L' measurement and is also in units of milliseconds. The ratio L/M gives a curve factor related to the shape of the transient voltage curve, and is a measure of the rate of decay of the transient voltage. This is of secondary diagnostic value in that the rate of decay of the transient voltage is partially a function of particle size. A large L/M ratio reflects a short time constant, commonly associated with finely disseminated sulphide or graphite, whereas a small L/M ratio reflects the longer time constants associated with the larger sized metallic particles.

The L/M ratio is also effective in determining the presence of electromagnetic coupling effects. With the Scintrex Induced Polarization unit, electromagnetic coupling effects are essentially eliminated by an 0.45 second delay-time following termination of the primary current pulse before measurement of the transient voltage commences. However, in extremely low resistivity areas coupling may occur. Under these conditions the presence of electromagnetic coupling can distort the Induced Polarization response, and it is extremely important to know when this occurs. The presence of such coupling is immediately recognizable from the L/M ratios.

Resistivity measurements are also made as an integral part of all Induced Polarization measurement using the Scintrex Induced Polarization unit. The resistivity values are of primary importance in determining subsurface geological features such as contact zones, faulting, etc., and are of assistance in mapping the geology in general.

Electrode geometries (see Figure 2) utilised in obtaining field measurements are important and no one electrode array is applicable for all conditions. In areas where a low resistivity oxidised surface layer overlies a much higher resistivity freshrock, a high degree of

COMMONLY USED ELECTRODE ARRAYS

CLOSE – COUPLED ARRAYS

DIPOLE – DIPOLE

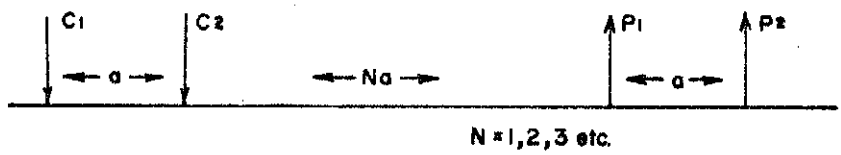

POLE – DIPOLE

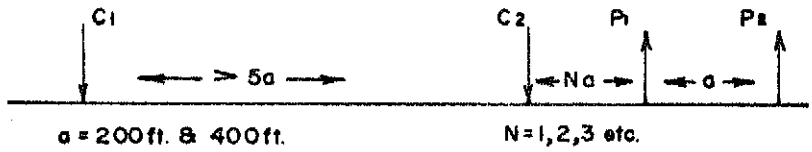

GRADIENT ARRAY

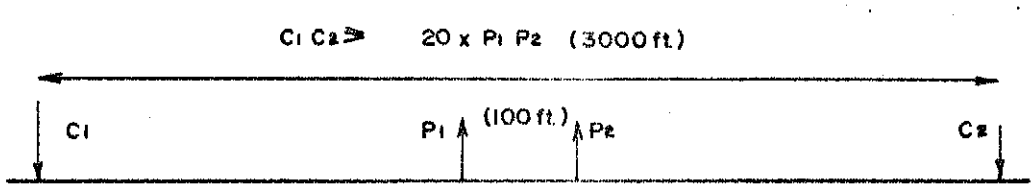

Fig. 2

masking occurs using any of the close-coupled arrays, such as pole-dipole or dipole-dipole. An electrode spacing many times greater than the depth to freshrock must be used in order to obtain responses reasonably representative of the freshrock. With such large electrode spacings the physical properties are effectively averaged over so large a volume that we lose the ability to detect moderate sized bodies of polarizable material. However, under these conditions the gradient array is both feasible and desirable in that it minimises the effects of masking and at the same time has a high degree of resolution for small targets.

In the present areas of investigation, abnormal induced polarization responses may be expected to arise from the electronically conducting sulphide minerals such as pyrite, pyrrhotite, chalcopyrite and pentlandite, plus graphite and magnetite. The response from magnetite has been found to be quite variable and somewhat unpredictable, reflecting the great variation in the mode of electrical conduction in this material. It is not always possible to differentiate between these potential sources of high chargeability from the Induced Polarization and resistivity data alone. Complementary geophysical, geochemical and geological data enable a more complete interpretation to be made of the Induced Polarization data.

REFERENCES

Seigel, 1962 — "Induced Polarization and Its Role in Mineral Exploration" H.O. Seigel, Canadian Mining and Metallurgical Bulletin, April, 1962.

ed. Wait, 1959 — "Overvoltage Research and Geophysical Applications" editor J.R. Wait, Pergamon Press, London, 1959.

APPENDIX 'T'

BRIEF DESCRIPTION OF THE TURAM ELECTROMAGNETIC SYSTEM

GENERAL

The Turam method can be classified as a fixed source compensation method. The primary or source field consists of a large energising layout in the form of a long wire or a large loop laid out on the terrain, to which an audio frequency alternating current is fed by means of a motor generator. The resulting current pattern is investigated inductively, with two identical receiving coils connected to a bridge compensator which compares the signal received in each coil in relative phase and amplitude. When grounded cable is used, the energisation is both galvanic and inductive; when the primary layout consists of a closed loop, the energisation is purely inductive. Under most conditions the presence of galvanic current is undesirable and inductive energisation, is as a rule, preferred.

Although the system allows the comparison of any two components of the resultant field, it is standard procedure on systematic surveys to measure the gradient of the vertical component.

The pattern for a typical Turam survey is shown in Figure 1. A large rectangular loop is used as primary

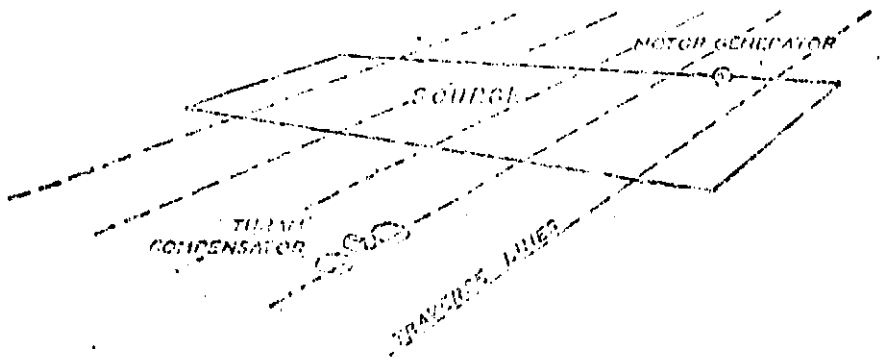

Fig. 1 The Turam method. General layout

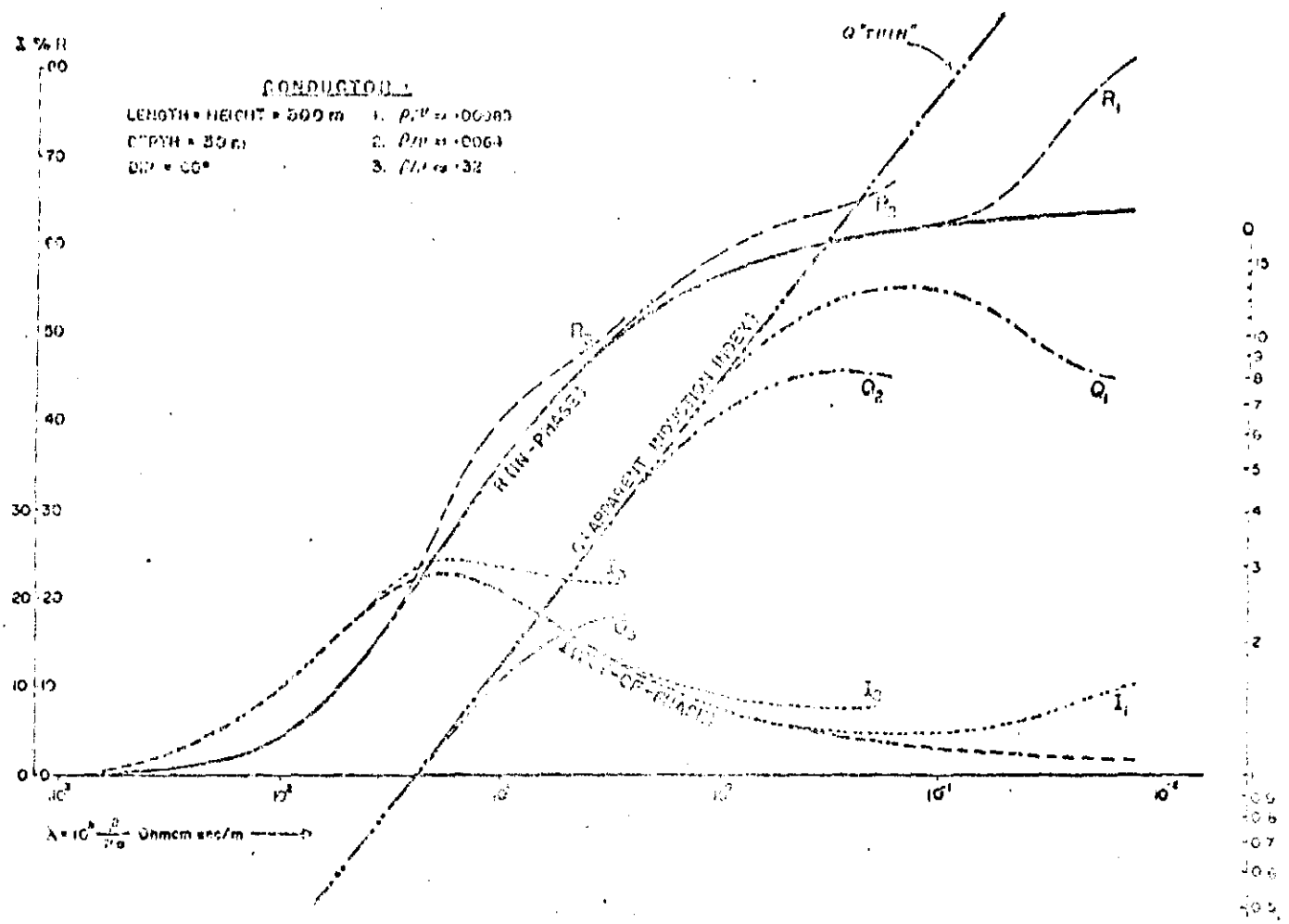

FIG. 2 RESPONSE OF A FINITE TABULAR CONDUCTOR.
(R.A. Bosschart 1964)

layout and the field gradients are measured with horizontal receiving coils along profiles perpendicular to a long side of the transmitting loop.

DATA REDUCTION

The relative strength of the undisturbed primary field is dependent on the loop dimensions and the location of the observation points, and can be determined by calculation. The measured field strength ratios are normalised through division by these calculated free space ratios.

The primary field causes eddy current to flow in subsurface conductors. As a result the resultant field will be distorted in both amplitude and phase. The presence of conductors will thus be indicated by abnormal strength ratios and phase differences.

PRESENTATION

The measuring results are usually presented in profile form as (reduced) field strength ratio and phase difference curves, with the observed values plotted at the midpoint between coil positions.

Occasionally one of the two parameters is presented in contour form, but contour plans are generally inadequate

to express the full significance of the data.

INTERPRETATION

Where field distortion occurs the curves indicate the location and the depth of burial of the main current flow. The "current axis" is well defined when the current is concentrated as, for instance, in thin, steeply dipping conductors. In wide, banded conductors or in horizontal conductors such as , for instance, overburden, the current is usually more dispersed and the anomalies will yield less positive information.

As a rule the current axis is located right below the maximum field strength ratio deflection or the maximum negative phase shift. Its depth under the traverse is indicated by the shape of the anomaly.

The relative amplitudes of field strength and phase distortions are a measure of the conductivity of the conducting bodies, i.e. good conductors are characterised by field strength distortion combined with relatively little phase shifting, whereas poor conductors affect the phase rather than the strength of the resultant field.

For an accurate grading the resistivity thickness (r/d) ratios of the individual conductors can be derived from the calculated in-phase and out-of-phase components, taking further into consideration the exciting frequency and the strike length of the conductor. The relations are shown in Figures 2 and 3. The obtained r/d values are marked on the upper right side of the anomalies, in units of ohmcm/m. On the lower left side the depth of the current axis (ft.) is marked. It is normally located 30 - 40 feet within the body and the indicated depth should be regarded as the maximum depth to the upper surface of the conductor.

To obtain the projection of the current pattern, the anomalies are connected between lines whereby depth and r/d values as well as other characteristics of the curves are used as criteria. The strike of the formations, if known, is also taken into consideration.

Figure 4 and 5 show a plan and section of a typical Turam survey and interpretation.

REFERENCES

1937, Hedstrom, E.H. Phase Measurements in Electrical Prospecting. AIME Tech. Publ. 827.

1964, Bosschart, R.A. Analytical Interpretation of Fixed Source Electromagnetic Prospecting Data. Delft.

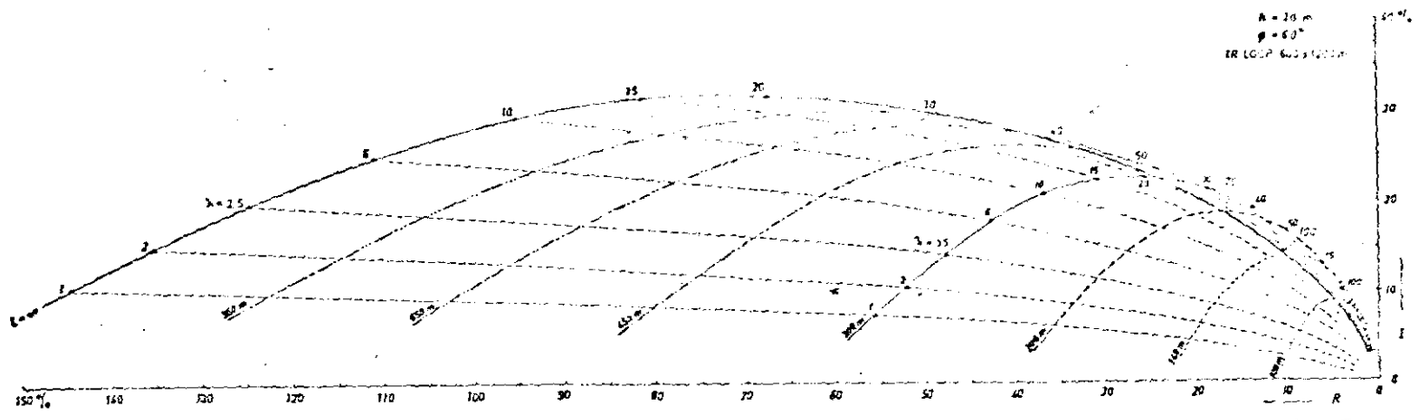

FIG. 3 RESPONSE DIAGRAM FOR CONDUCTORS OF VARYING STRIKE LENGTHS.

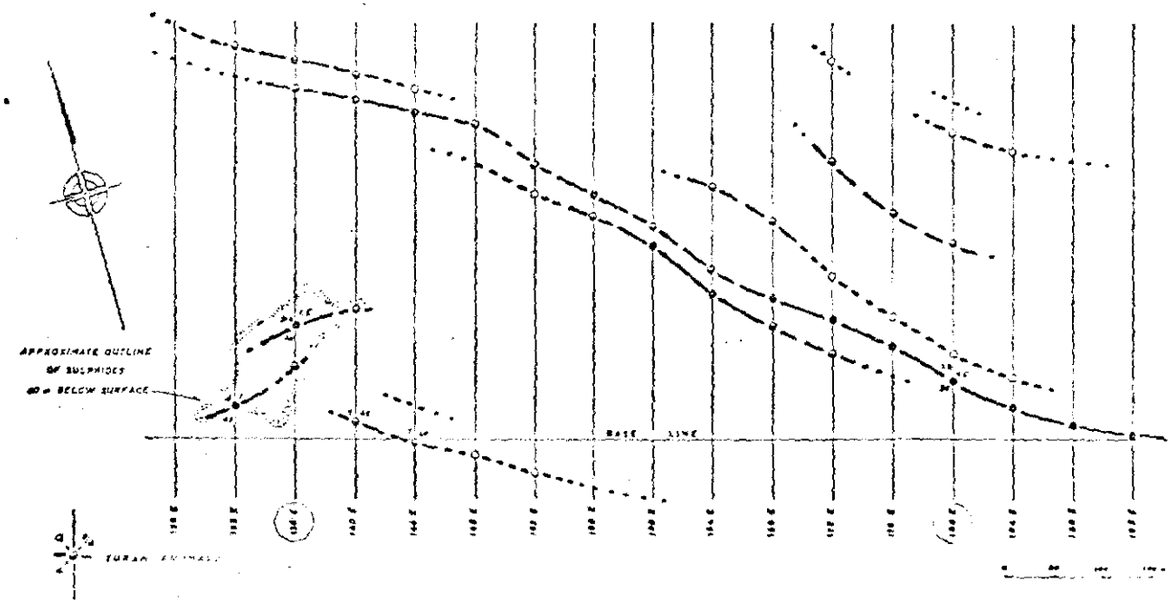

FIG. 4 TURAM SURVEY ON THE MURRAY GROUP, NEW-BRUNSWICK.
(R.A. Bosschart 1964)

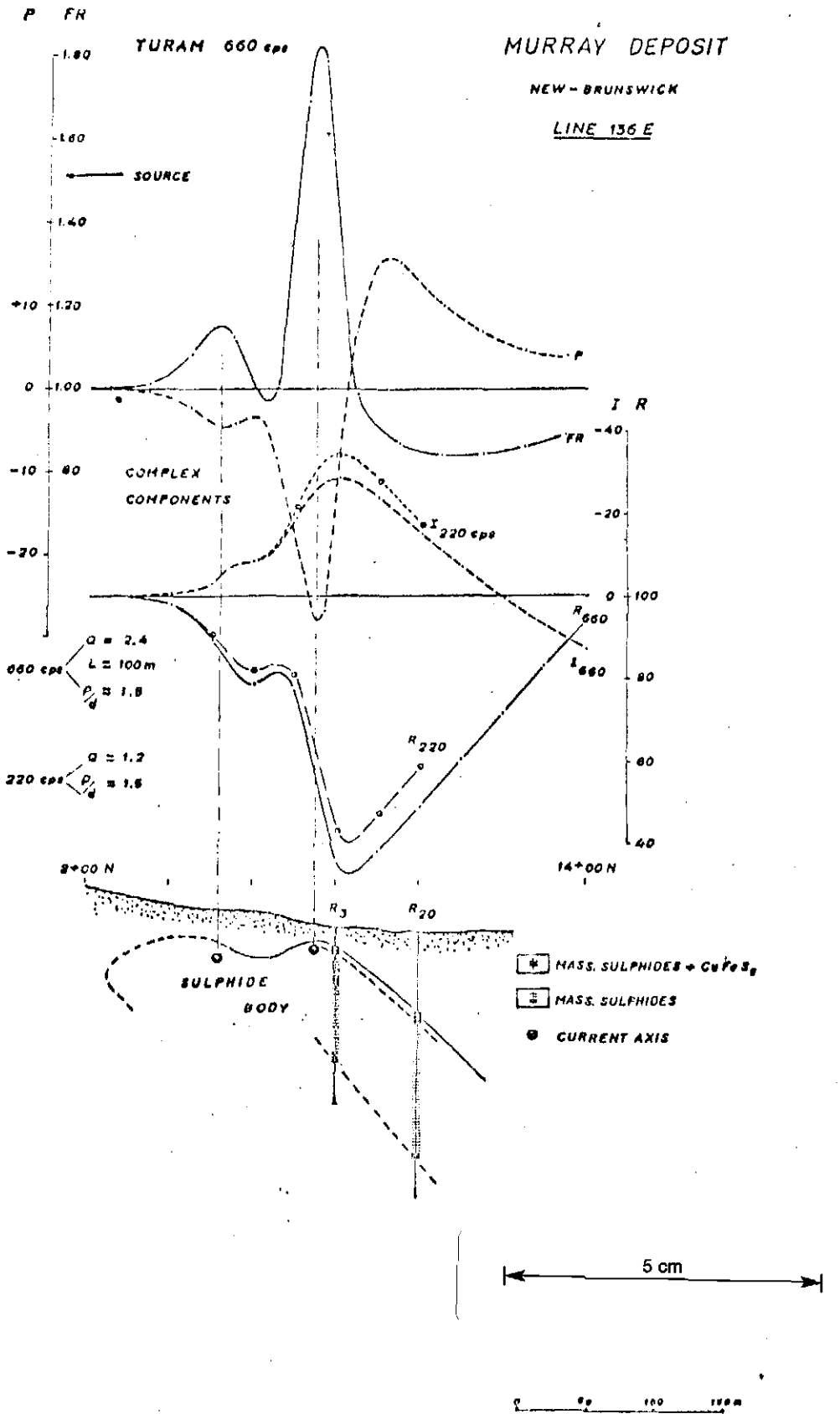

FIG. 5 TURAM SURVEY ON THE MURRAY GROUP, NEW BRUNSWICK. INTERPRETATION OF A TYPICAL SECTION. (R.A. Bosschart 1964)

APPENDIX 'MIP'

MAGNETIC INDUCED POLARIZATION

The MIP method measures the magnetic response due to the polarization currents flowing in the ground that are made up of the fundamental polarization current within the chargeable body and its return currents. Being able to measure the magnetic field due to the polarization current within the chargeable body a far more fundamental measurement with associated characteristics is obtained. The polarization current within the body is very concentrated and is in the opposite sense to the inducing current and the return current.

The magnetic field due to the inducing current shows where the primary current is flowing and hence where conductive or resistive zones are.

FIELD PROCEDURE

A longitudinal current array is normally applied so that the current is passed along the long axis or strike direction of sulphide bodies likely to be encountered in the survey area. A fixed current electrode configuration is employed with current electrodes separated by 2A where A is the minimum length of bodies desired to locate in the survey area. If there is one well defined horizon of interest then the current electrodes are normally placed reasonably on this line. The cable joining the current electrodes may be the shortest

distance between them or when a single well-defined horizon of interest is present, then the current is layed in a U shape avoiding the horizon. In this way the magnetic field from the cable will not obscure the favourable horizon.

With a current electrode separation of 2A, a block about 2A long x A wide may be covered. This is not a rigid limitation, however, and they may be exceeded somewhat providing the magnetic field has an adequate strength.

The horizontal magnetic field at right angles to the current flow is measured, that is, along the direction of the survey line. The distance between stations may vary between 25 and 60 metres depending on the size of body of interest and its depth.

The primary current into the ground is a standard two seconds on-off wave form. Using the IPR-8 receiver, the primary magnetic field H_p due to the primary current I_p flow in the ground is measured. When this is switched off, the decaying secondary current produces a secondary magnetic field H_s. The IPR-8 receiver can measure up to six slices in the decay curve produced by the secondary magnetic field, as shown in Appendix IPR-8. Each slice

is normalised for a standard decay curve, and the primary magnetic field, to give the chargeability parameter. The chargeability with the induced polarization phenomena is defined as the constant relating the primary to the secondary magnetic field, or current or electric field depending on what measuring technique is applied.

APPENDIX IPR-8

I INTRODUCTION

The basic equipment required for an Induced Polarization survey consists of a transmitter, a receiver, wire and electrodes.

Most time domain induced polarization transmitters transmit square waves with equal "on" and "off" times. Polarity is automatically changed between the pulses. The waveform shown below indicates how the current is usually transmitted. The pulse times range from 1 to 8 seconds.

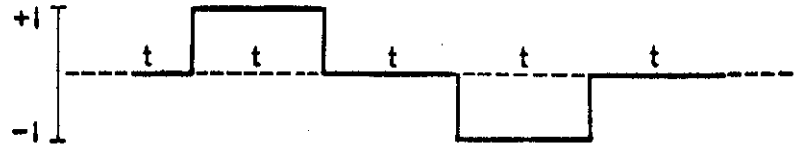

FIGURE 1A

The transmitter is powered by batteries (portable type units or a motor driven generator. Scintrex manufactures various time domain induced polarization transmitters ranging in power from 25 watts to 15 kW. The choice of a transmitter depends on various factors such as: the electrode spacings to be employed, contact resistance and the resistivity of the subsurface. The IPR-8 receiver is designed for use with any time domain induced polarization transmitter.

The IPR-8 time domain induced polarization receiver is of the state-of-the-art design, packaged in a rugged and portable manner. Using integration and automatic normalization, it measures the characteristics of an induced polarization decay curve set up by overvoltage and other effects occurring in rocks. When induced polarization effects (such as due to metallic-non metallic interfaces in rocks) occur, the waveform received at the receiver is not the same square wave as transmitted by the transmitter. The waveform shown below indicates the sort of wave distortion which is caused by the induced polarization phenomena.

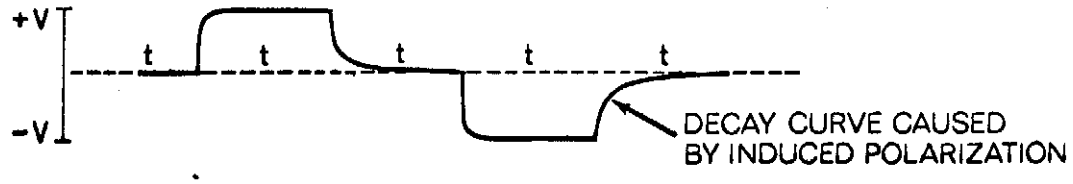

FIGURE 1B

II SPECIFICATIONS

The IPR-8 has the following specifications:

Input Impedance	3 megohms
Primary Voltage (Vp) Range	300 microvolts full scale to 40 volts full scale in 10 ranges
Accuracy of Vp Measurement	±3% of full scale
Vs/Vp Ranges	20 and 100 mV/V full scale
Vs/Vp Accuracy	±3% of full scale
Primary SP Buckout Range	±1 volt
Accuracy of SP Measurement	±3%, ±5 mV
Automatic SP Tracking Range	6 x Vp, maximum ±1 volt
Continuity Meter Reading	0 - 500 k ohms
50 or 60 Hz Powerline Rejection	-50 db (300x)*
Low Pass Filter	6 db/octave with fc = 20 Hz and 12 db/octave with fc = 36 Hz
Required Stability of Transmitter Timing	Need only exceed measuring program selected (1 or 2 seconds)
Operating Temperature Range	-30°C to +60°C
Dimensions	320 mm x 135 mm x 160 mm
Weight, Complete with Lid and Batteries	3.6 kg
Power Supply	4 D cells - Eveready No. 1050 or equivalent; estimated battery life 2 months intermittent duty at 25°C 1 Alkaline cell Eveready No. E91 or equivalent; estimated life 1 year

* 50 or 60 Hz depending on power system.

III QUANTITIES MEASURED BY THE IPR-8

Figure 2 shows the different parameters measured by the IPR-8. The usual measurements are Vp, the received primary voltage and "M", a parameter related to the transient curve. The Vp measurement is used in resistivity calculations while M is the chargeability (induced polarization) parameter. In addition, absolute values of the self-potential (SP) can be measured.

In all cases, the M quantity measured by the IPR-8 is the mean value of the transient voltage over a selected time interval to which the following normalizations have been applied:

- normalization for the length of the integration interval
- normalization for the primary steady state voltage (Vp)
- normalization for curve shape
- normalization for number of pulses

The units of the quantities measured are, therefore, dimensionless and are normally expressed in "millivolts per volt".

In the various modes of operation the transient voltage following the interruption of the primary current pulse is either integrated over one long period of time or sliced into either 3 or 6 slices. By using 6 slices, a good record of the decay curve shape can be obtained. The 3 slice mode gives some curve shape information and provides an economical standard mode in which to operate. The centre slice of this mode is reasonably close to the measurement made by the Scintrex IPR-7 and other receivers of the "Newmont Type", while the first and last slices can be used for a rapid check of curve shape. A more precise relationship is, however, presented later in this section.

Figure 2 shows the actual times used. For the receiver to operate, the transmitter timing may be any time period of one second or greater (i.e. $t \geq 1$ second) although transmitter and receiver timings of 2 seconds are considered normal for most surveys. Equal on and off timing assures the best noise rejection as the signal is averaged over the longest possible time, and the automatic self-potential adjustment is made closest to the reading time.

With the receiver set at t = 1 second, the decay ($\delta/2$) from the current-off time to the commencement of the measurement is 65 milliseconds and the slice width (δ) is 130 milliseconds. With the receiver set at t = 2 seconds the delay is 130 milliseconds and the slice width is 260 milliseconds. Fuller information on the programs is available from the tables in Figure 2.

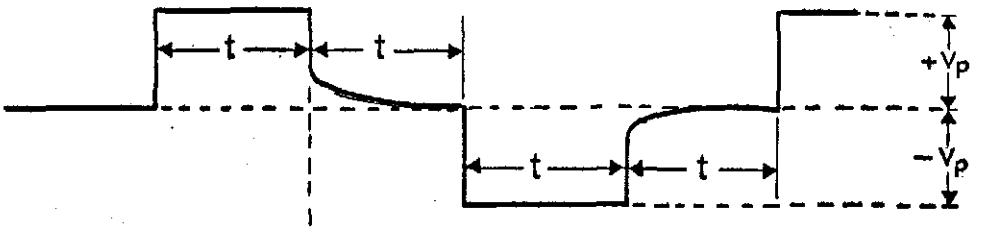

WAVE FORM AT INPUT TERMINALS

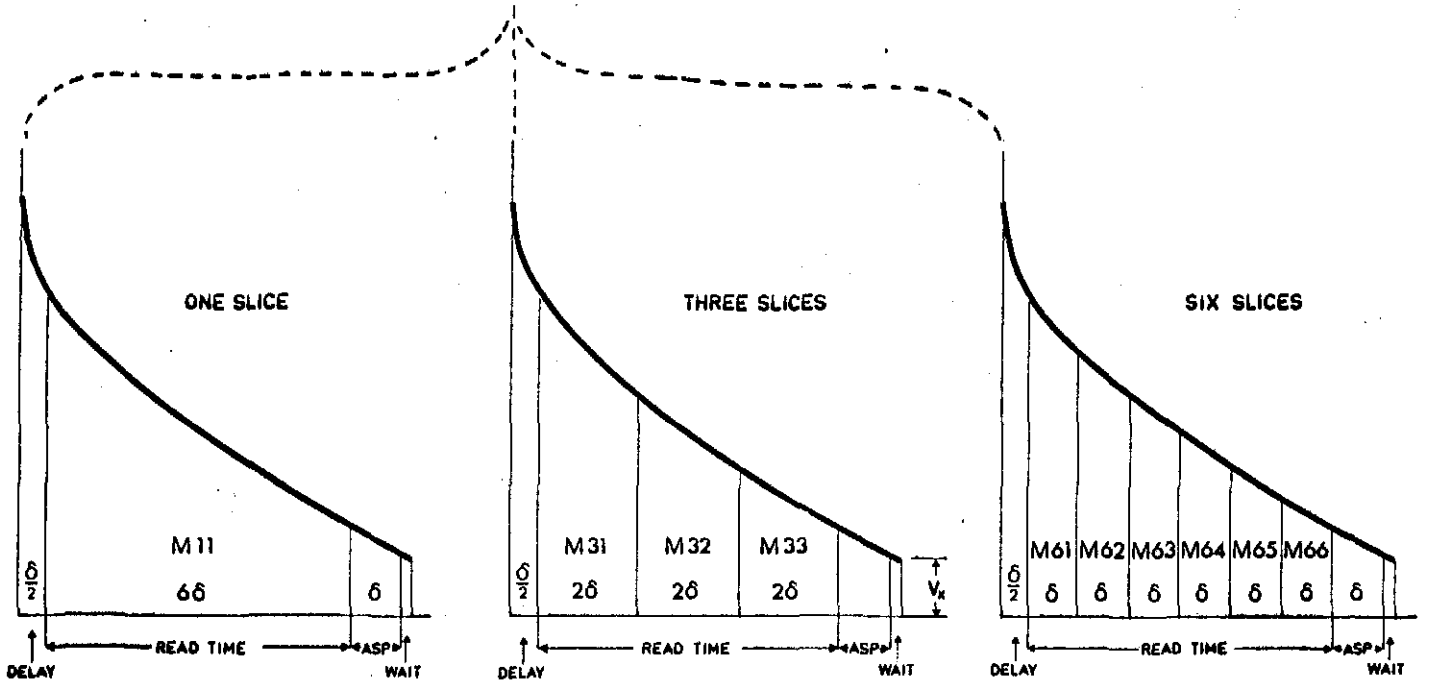

SECONDARY DECAY CURVE SHAPES AS APPLIED TO THE INTEGRATORS

t sec.	δ	delay time	waiting time	M 11				M 31			M 32			M 33			length
				from	to	mean	length	from	to	mean	from	to	mean	from	to	mean	
1	130	65	25	65	845	455	780	65	325	195	325	585	455	585	845	715	260
2	260	130	50	130	1690	910	1560	130	650	390	650	1170	910	1170	1690	1430	520

t sec.	M 61			M 62			M 63			M 64			M 65			M 66			length
	from	to	mean	from	to	mean	from	to	mean	from	to	mean	from	to	mean	from	to	mean	
1	65	195	130	195	325	260	325	455	390	455	585	520	585	715	650	715	845	780	130
2	130	390	260	390	650	520	650	910	780	910	1170	1040	1170	1430	1300	1430	1690	1560	260

FIGURE 2

PARAMETERS MEASURED WITH TIMES OF RECEIVER PROGRAM IN MILLISECONDS.

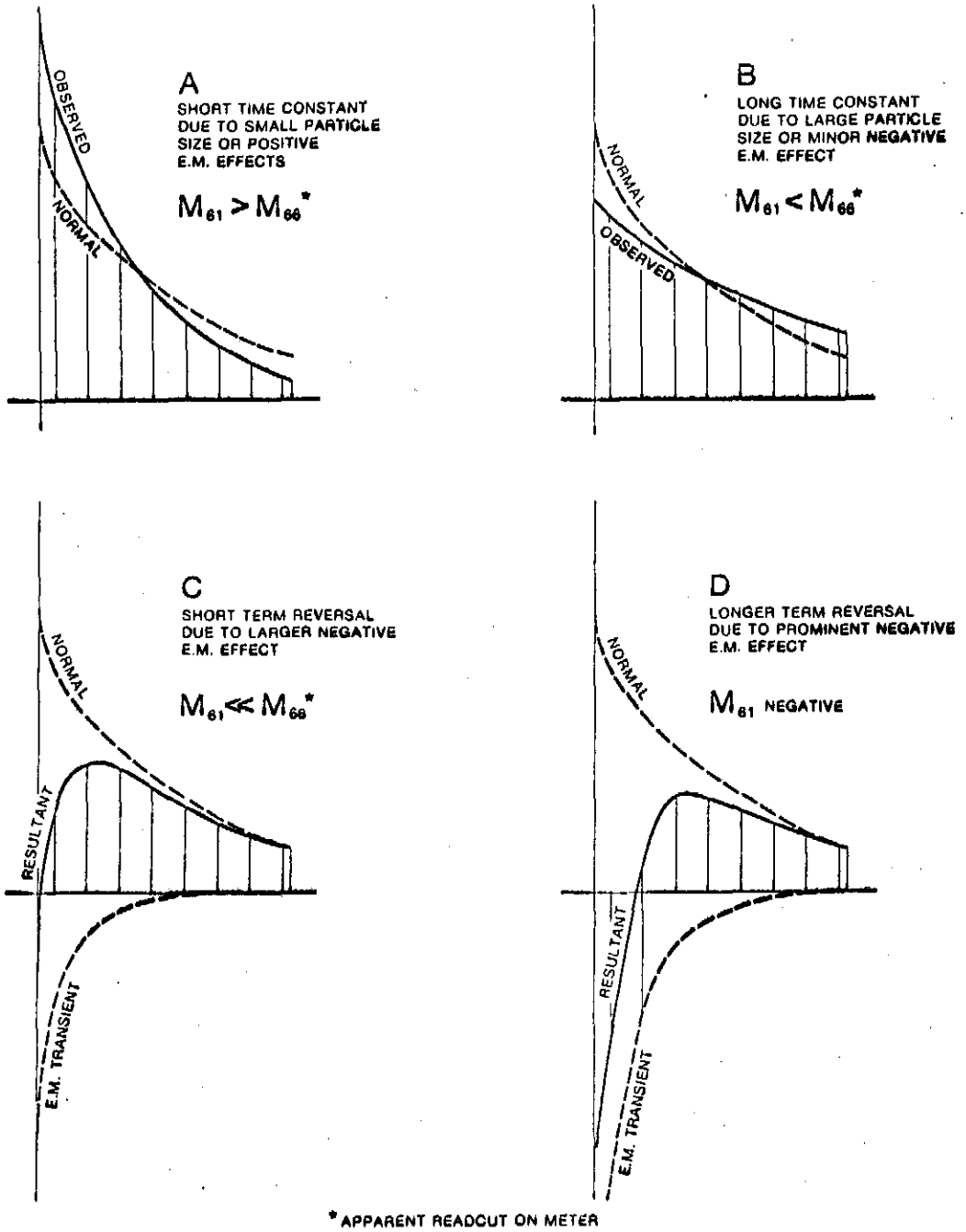

*APPARENT READOUT ON METER

FIGURE 3

THE SIGNIFICANCE OF CURVE SHAPE INFORMATION GAINED USING 6 SLICE READINGS.

Each integration is normalized with respect to the Standard Induced Polarization Decay Curve which has been established by Newmont Exploration Limited. (ref. Dolan and McLaughlin in bibliography) This is achieved by choosing the sensitivities of the integrators so, that if the curve shape is normal, all slices within a given mode show the same amplitude of measurement. A further normalization is built in for the slice width, be it full, one-third or one-sixth of the total integration period. The net effect is that the reading will be the same regardless of the slice measured, providing that a standard transient decay curve form is present and that the same measuring cycle is used for transmitter and receiver (1 second or 2 seconds). Any departure from this standard curve form will be immediately obvious to the operator, without performing any calculations. For instance, a steeper decay will give a higher reading on earlier slices than on later slices. Reconstruction of the actual decay curve is easily effected by using the correction factors given in Table 1.

The shape of a time domain induced polarization decay curve can be altered by electromagnetic or interline coupling, by variations in the average size or degree of interconnection of the metallic particles in the bedrock or by other I.P. sources. Figure 3 illustrates the advantage of breaking the decay curve into slices. Utilizing only one wide slice, there is no indication of the shape of the decay curve. Positive electromagnetic coupling effects or small particle size may give rise to an abnormally short time constant (Case A) which, for multi-slice modes will be indicated by higher normalized readings of the earlier slices with respect to the later slices. An increase in the later slices over the earlier ones (Case B) may imply a longer time constant due to a minor negative EM transient or I.P. responses from large metallic particles, etc. Cases C and D, where the values of the initial slices are considerably reduced or are even negative, show the effect of negative EM transients of increasing amplitude.

A system of symbols has been created to indicate each of the measurable slices.

The general symbol is M_{txy} where:

- t is the timing chosen (i.e. 1 or 2 seconds)
- x is the number of slices in the mode chosen (i.e. 1, 3 or 6)
- y is the number of the slice referred to (i.e. 1, 2, 3, 4, 5 or 6)

Wherever two subscripts only are given, eg. M_{32}, it is understood to apply equally for t = 1 sec. or t = 2 sec.

A chargeability reading is defined by the following formula:

$$M = \frac{V_s \cdot 1000}{V_p} \quad \text{in mV/V}$$

where $$V_s = \frac{t_1 \int^{t_2} V_s \, dt}{t_r} + V_x$$

and t_1 = time at beginning of slice

t_2 = time at end of slice

V_x = residual transient voltage at the end of the automatic self potential correction

$t_r = t_2 - t_1$, i.e. the integrating period

Chargeability values, uncorrected for curve shape, can be easily calculated if required. Normalizations for all slices are made using the M_{232} value as reference. In other words, there is no curve shape normalization applied to this slice; the M_{232} readout is, therefore, directly as measured. The same statement holds for the M_{132} slice, however, its value is one-half the value for M_{232} provided that the transmitter timing matches the receiver timing.

To restore the true transient curve shape (M true), the observed M readings (M read) are multiplied by the factors in Table 1.

TABLE 1

$$M_{true} = M_{read} \cdot k_1$$

Slice	k_1	
M_{11}	1.09	
M_{31}	1.47	
M_{32}	1.00	← NORMAL
M_{33}	0.81	
M_{61}	1.68	
M_{62}	1.27	
M_{63}	1.06	
M_{64}	0.94	
M_{65}	0.85	
M_{66}	0.78	

For the ideal "normal" I.P. transient curve form $M_{2xy} = 2M_{1xy}$ where M_{2xy} is for a 2-second on-off transmitter cycle and M_{1xy} is for a 1-second on-off cycle. The relationship between readings taken with differing transmitter and receiver timings is more complicated, particularly if the curve shapes are not normal.

Table 1 still applies for the case where the transmitting times are longer than the receiving times in order to reconstruct the relative curve shape.

Relationship between IPR-8 and
"Newmont Type" Receiver Measurements

The "Newmont Type" receivers (eg. Scintrex IPR-7) integrate the area under the transient curve from 0.45 seconds to 1.1 seconds. This is then multiplied internally be an instrumental factor to obtain the chargeability M in milliseconds.

For a normal decay curve form, the approximate relationship between the IPR-8 measurements and the Newmont Type chargeability is given by M_{232} (in mV/V) = M_N (in milliseconds) • 0.7.

REPORT ON

DETAILED ELECTRICAL GEOPHYSICAL SURVEYS

MT. TYNDALL AREA, NEAR QUEENSTOWN, TASMANIA

ON BEHALF OF

THE MOUNT LYELL MINING AND RAILWAY COMPANY LTD.

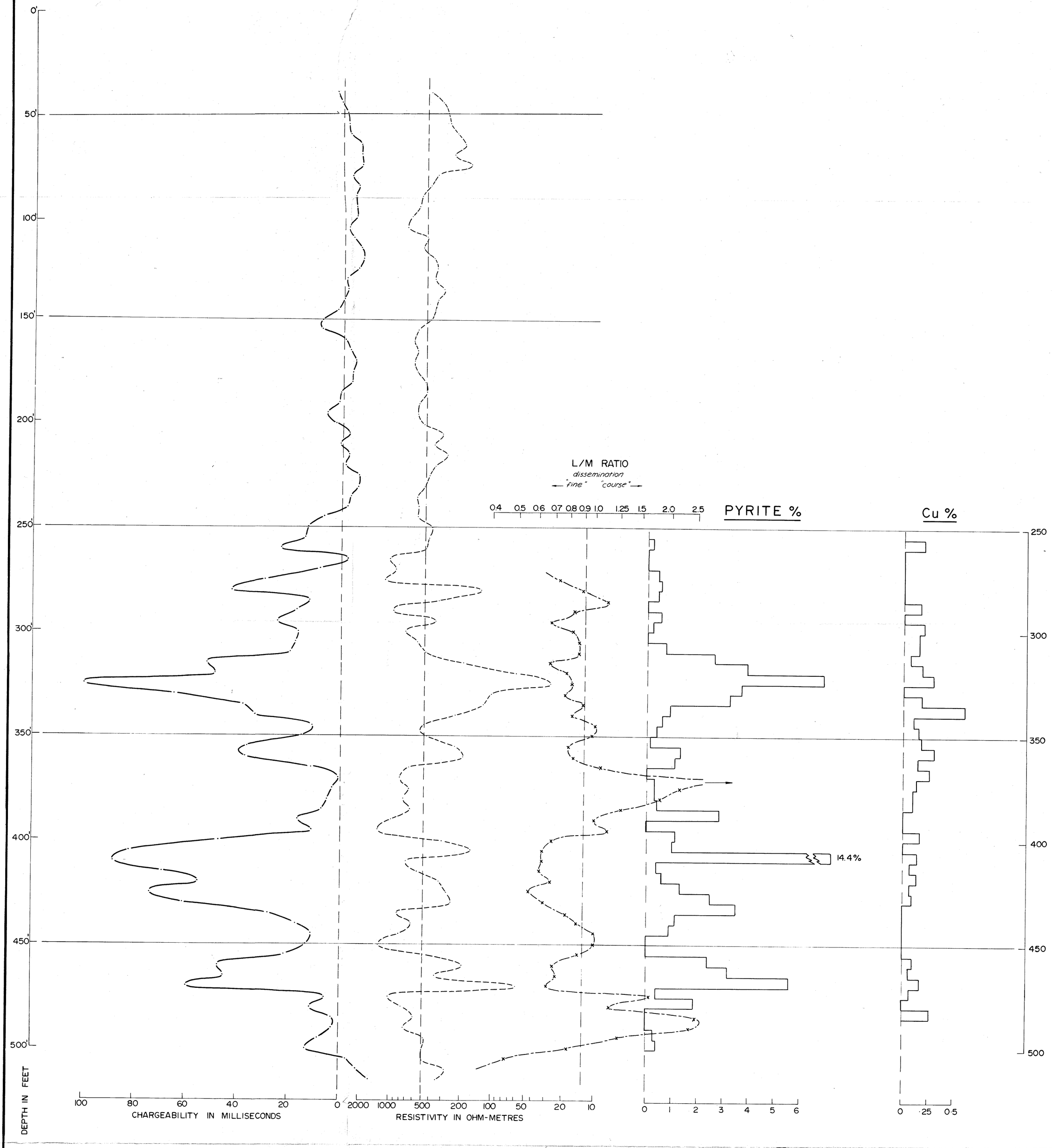

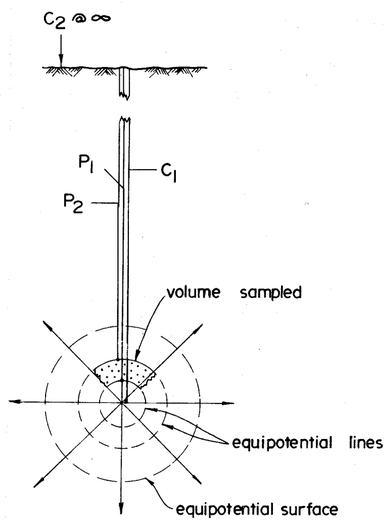

THE MOUNT LYELL MINING AND RAILWAY COMPANY LTD.

MT. TYNDALL AREA WEST COAST TASMANIA

5 FT. THREE ARRAY LOG DDH HFZI, LINE 63

324073

SURVEYED AND COMPILED BY
SCINTREX PTY. LTD.

DECEMBER 1973

043

84-2236 vol 2.

JOB No. TAS. 018 C SHEET 1 of 1 PLATE 1

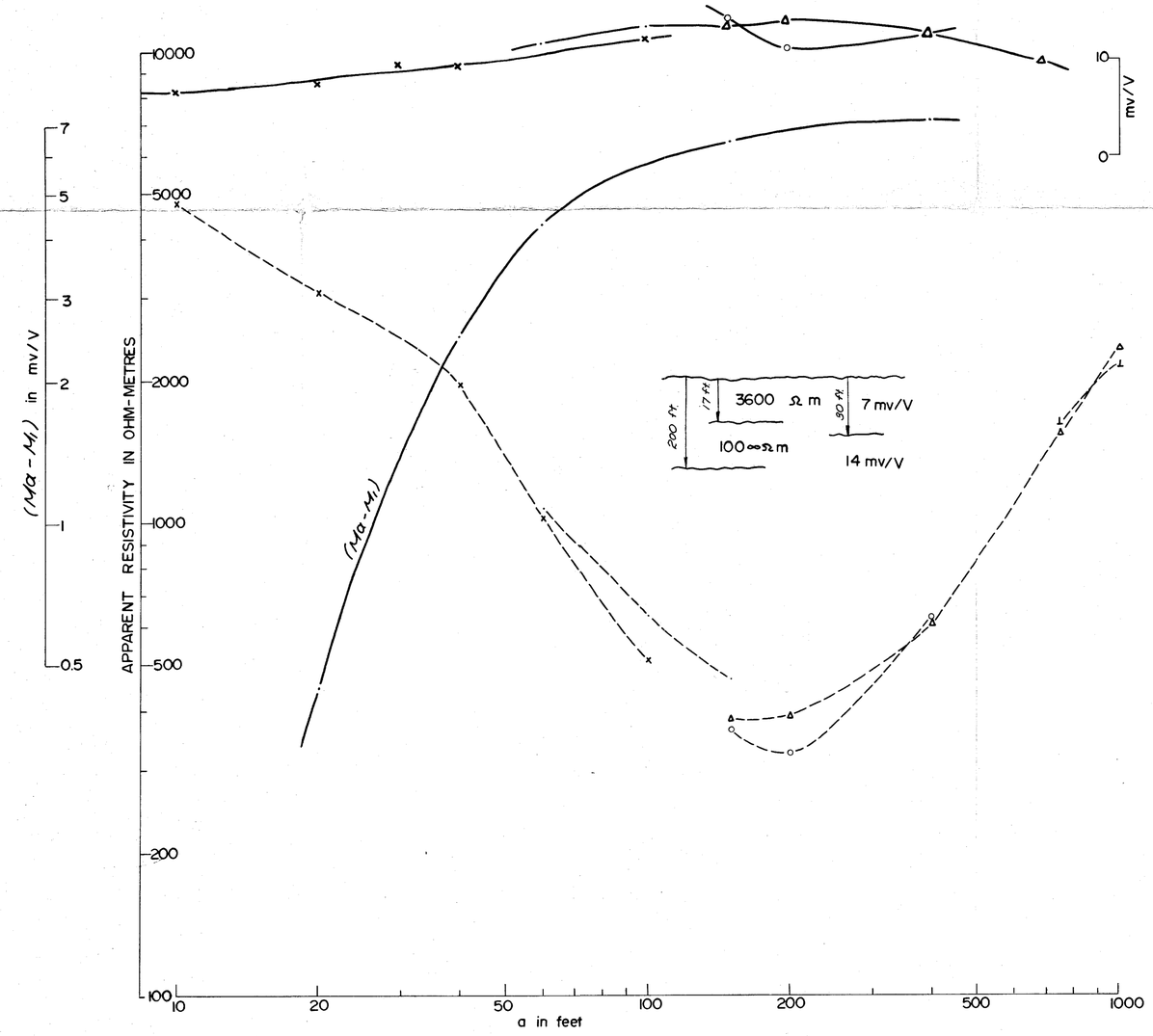

LINE 56 at 00

x — x — x b = 3
· — · — · b = 5
○ — ○ — ○ b = 10
△ — △ — △ b = 25
⊥ — ⊥ — ⊥ b = 50

THE MOUNT LYELL MINING AND RAILWAY COMPANY LTD.

MT. TYNDALL AREA
WEST COAST TASMANIA

SCHLUMBERGER ELECTRICAL SOUNDING

324074

SURVEYED AND COMPILED BY

SCINTREX PTY. LTD.

MARCH, 1974

044

84-2236 vol 2

JOB No. TAS. 018 C SHEET 1 of 1 PLATE 2

Line 52 N

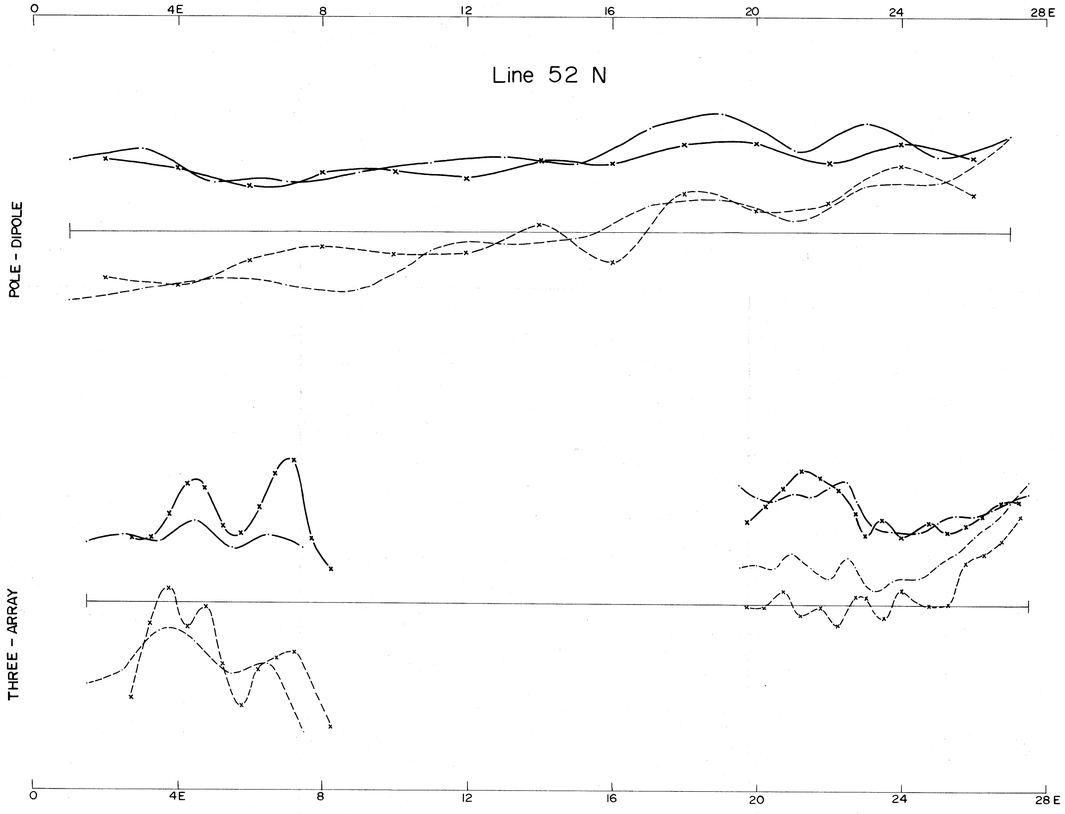

Line 53 N

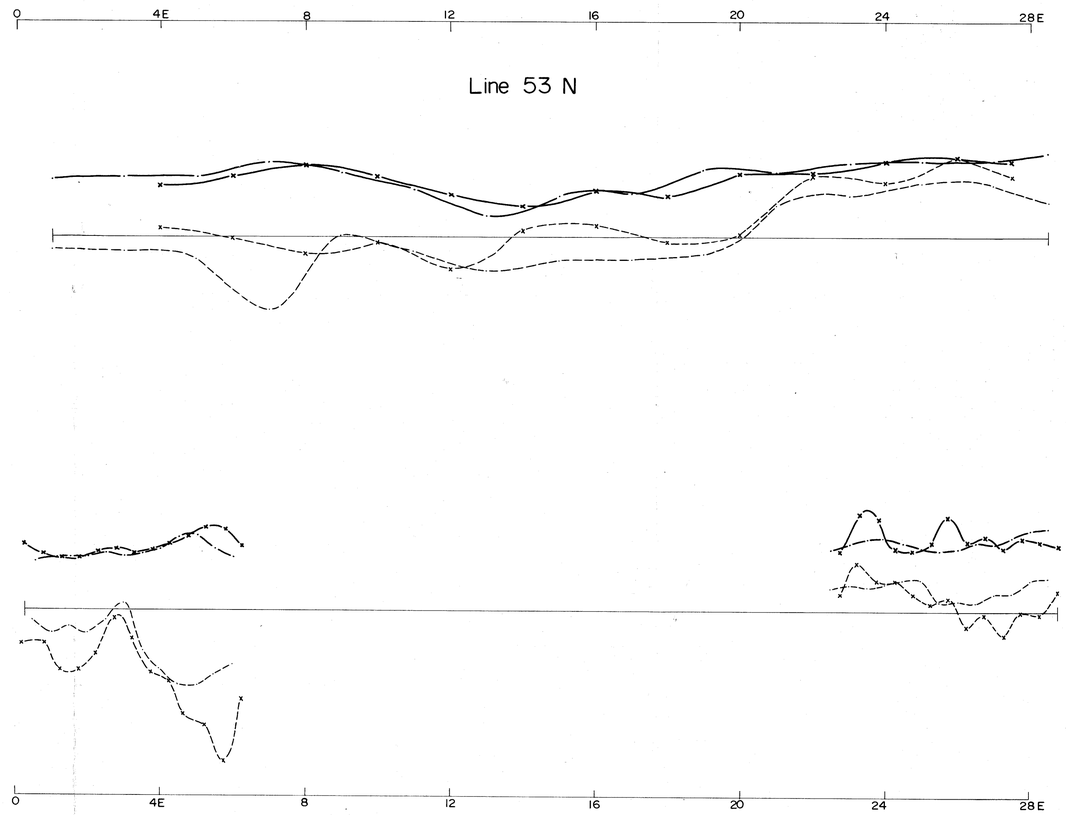

THREE ARRAY (to scale)

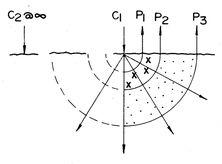

$P_1 - P_2$, a = 50' x—x

$P_2 - P_3$, a = 100' ·——·

POLE - DIPOLE (to scale)

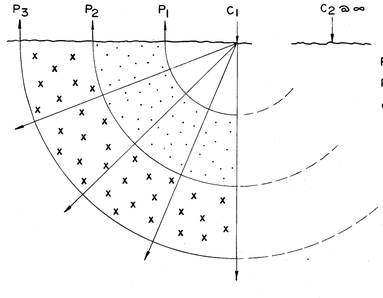

$P_1 - P_2$, n = 1 ·——·

$P_2 - P_3$, n = 2 x——x

a = 200

LEGEND

CHARGEABILITY SCALE, 1" = 10 millivolts / volt
BASE LEVEL = 0
SYMBOL = ·——x——·——x

RESISTIVITY SCALE, 2" = 1 logarithmic cycle
BASE LEVEL = 2000 Ohm-metres
SYMBOL = ·——·——x——·——·

THE MOUNT LYELL MINING AND RAILWAY COMPANY LTD.

MT. TYNDALL AREA
WEST COAST TASMANIA

ELECTRICAL INDUCED POLARIZATION SURVEY
CLOSE COUPLED ARRAY DETAIL
DATA PROFILES

324075

SURVEYED AND COMPILED BY
SCINTREX PTY. LTD.

5 cm

200 0 200 400 feet
Scale 1:2400

84-2236

JOB No. TAS. 018 C SHEET 1 of 1 PLATE 3

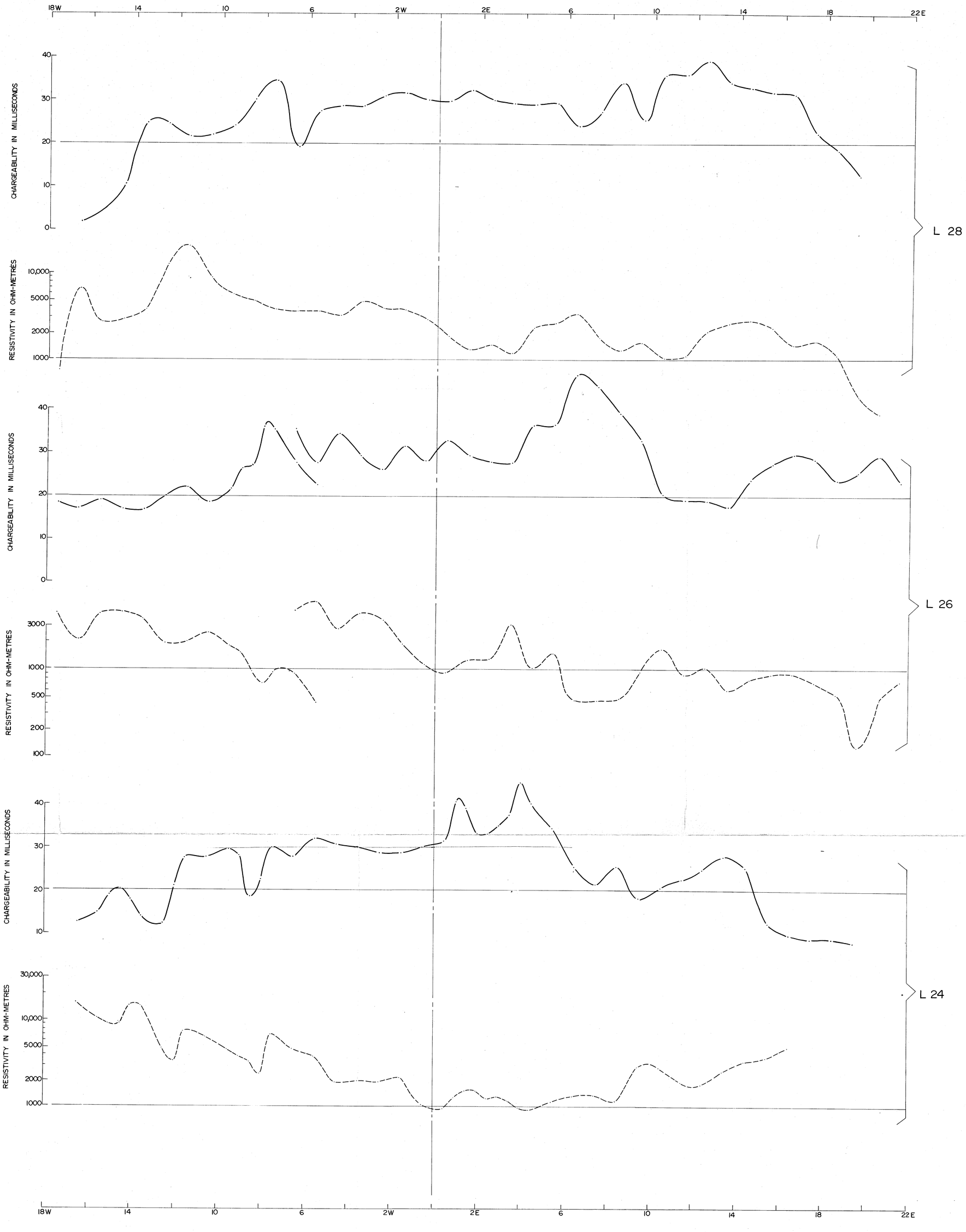

THE MOUNT LYELL MINING AND RAILWAY COMPANY LTD.

WEST-GRID
MT. TYNDALL AREA
WEST COAST TASMANIA

GRADIENT ARRAY DETAIL
DATA PROFILES

324076

5 cm

SURVEYED AND COMPILED BY
SCINTREX PTY. LTD.

DECEMBER 1973

200 0 200 400 feet
Scale 1:2400

JOB No. TAS. 018 C SHEET 1 of 1 PLATE 4

84-2236 vol 2.
046

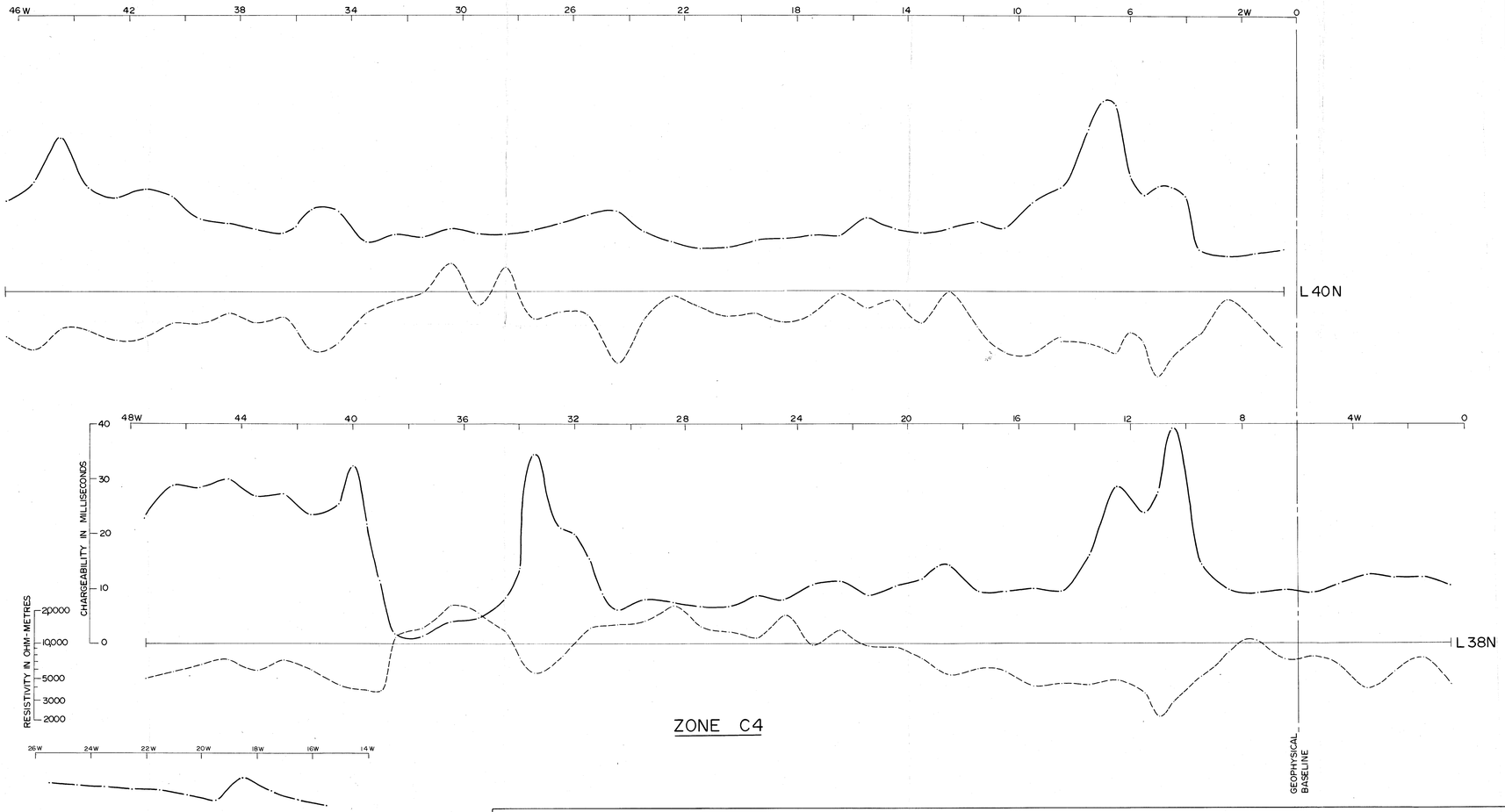

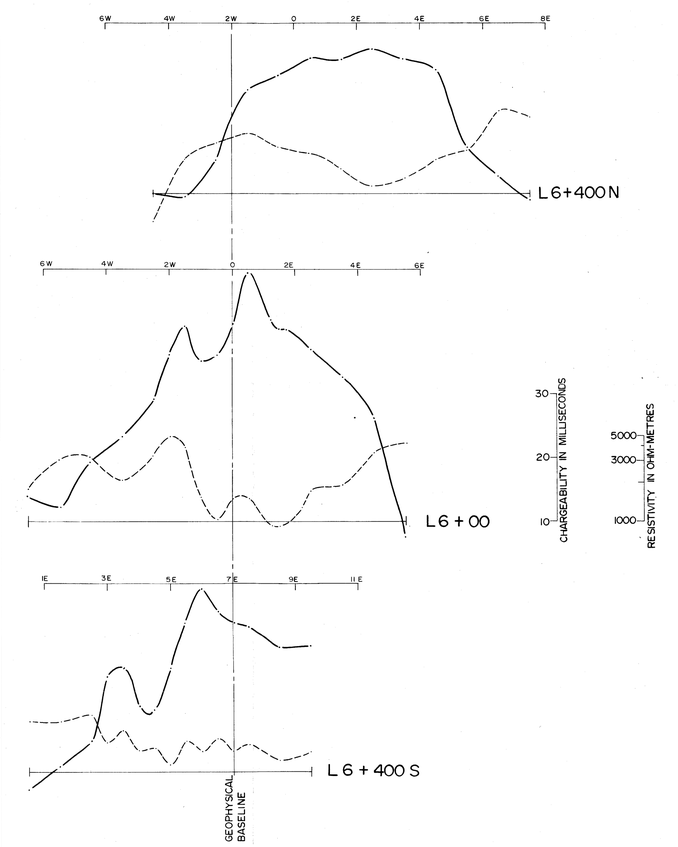

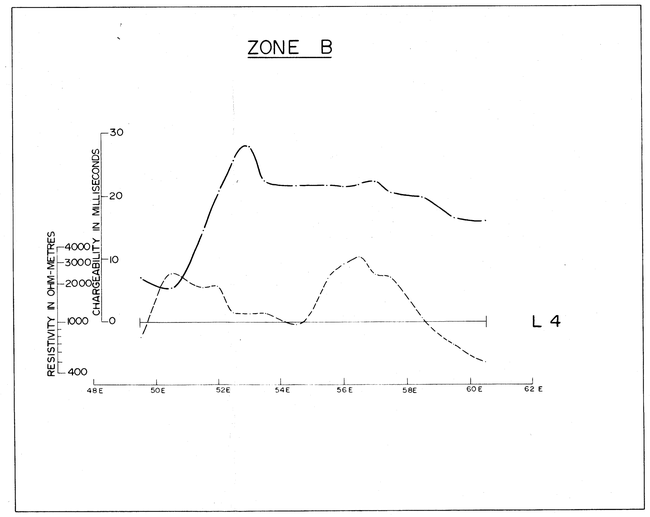

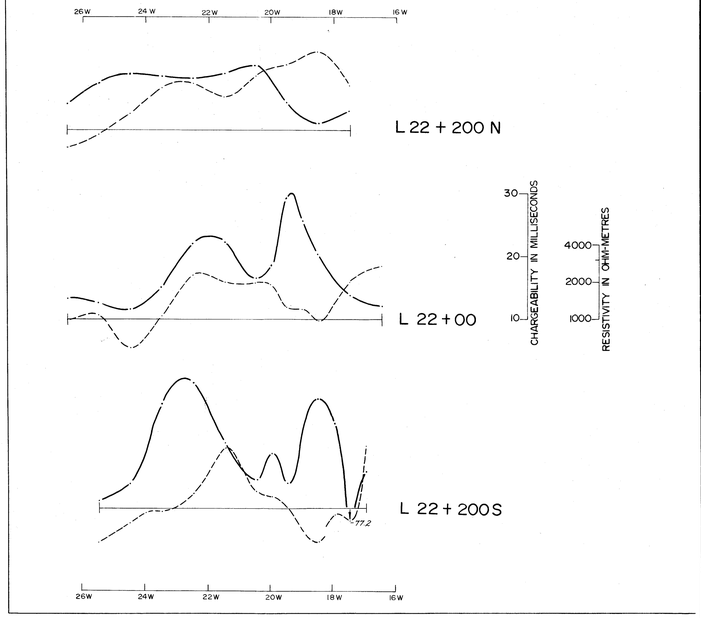

LEGEND

CHARGEABILITY SCALE 1" = 10 Milliseconds

SYMBOL = · —— · ——

RESISTIVITY SCALE 2" = 1 Logarithmic cycle

SYMBOL = · - - - · - - -

THE MOUNT LYELL MINING AND RAILWAY COMPANY LTD.

EAST-GRID
MT. TYNDALL AREA
WEST COAST TASMANIA

GRADIENT ARRAY DETAIL
DATA PROFILES

324077

5 cm

SURVEYED AND COMPILED BY
SCINTREX PTY. LTD.

DECEMBER 1973

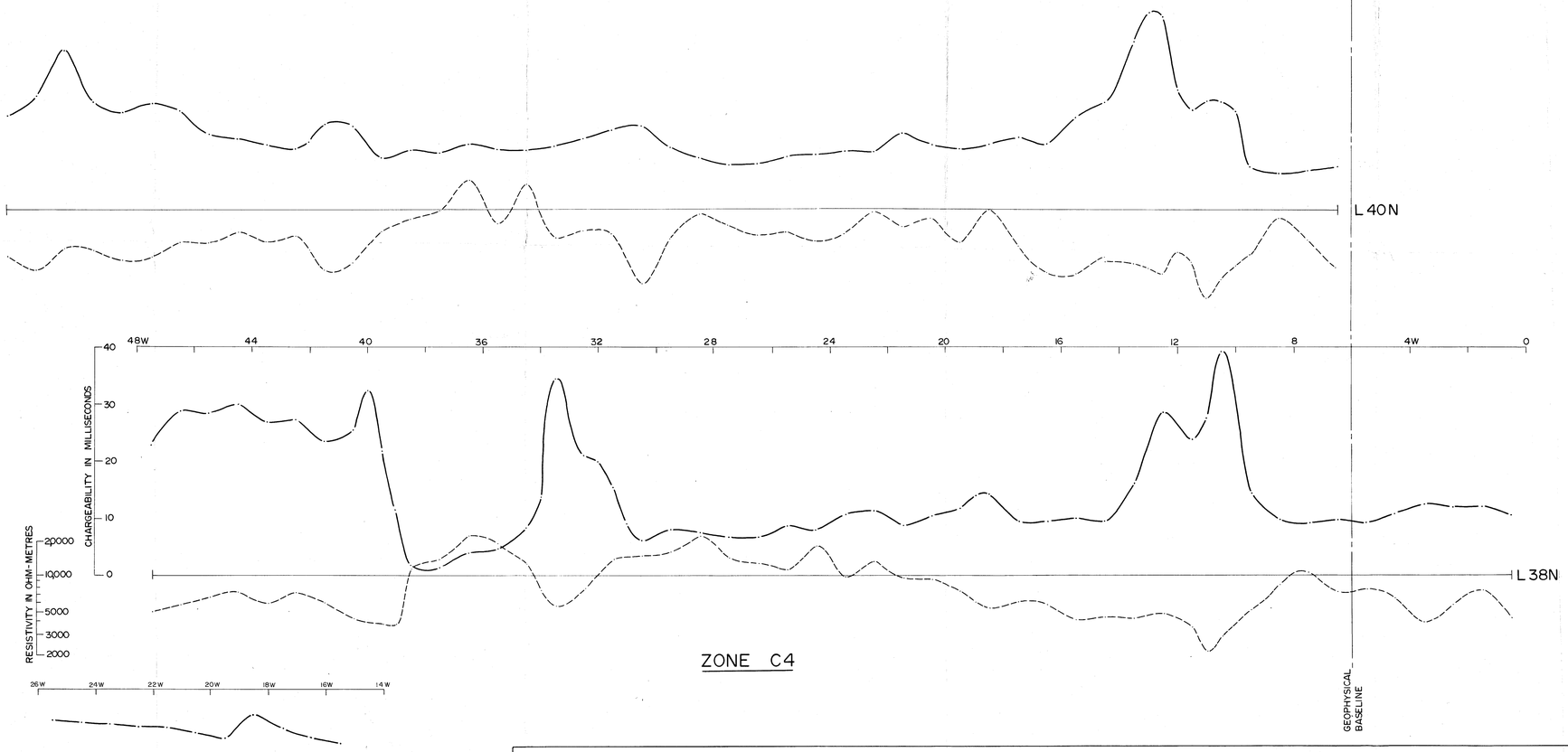

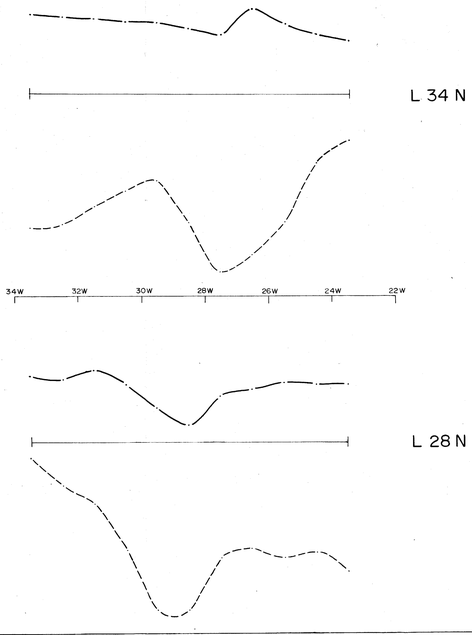

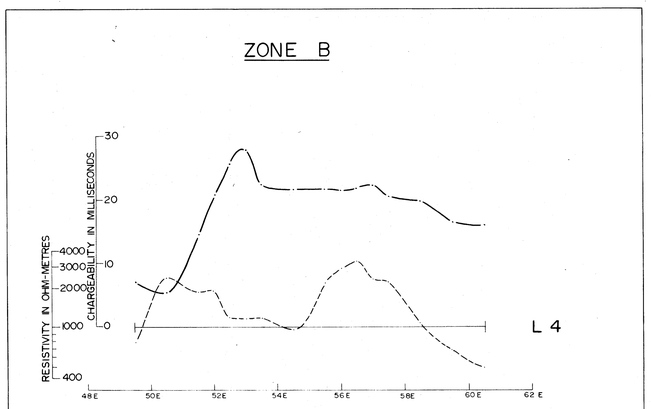

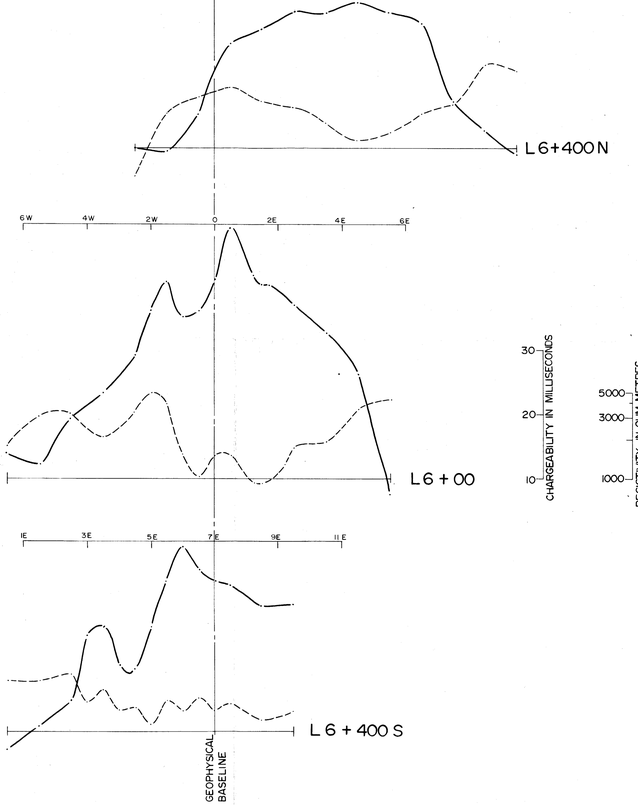

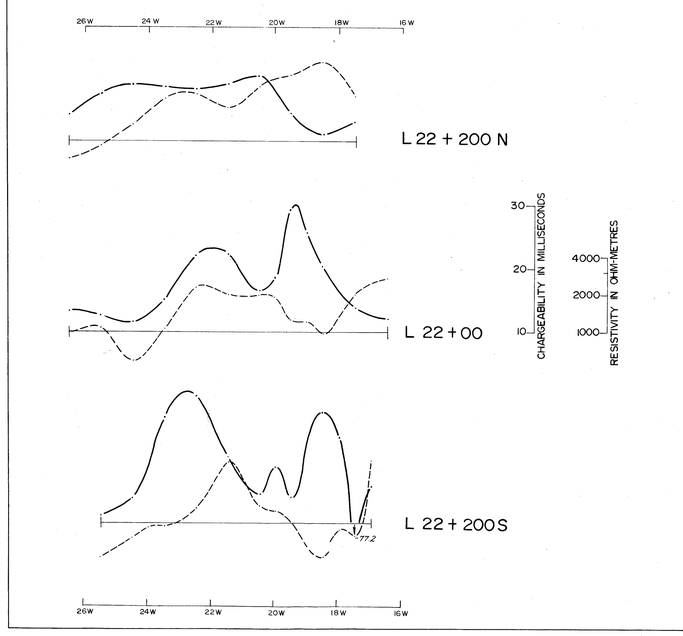

LEGEND

CHARGEABILITY SCALE 1" = 10 Milliseconds

SYMBOL = · ——— · ———

RESISTIVITY SCALE 2" = 1 Logarithmic cycle

SYMBOL = – – – · – – –

THE MOUNT LYELL MINING AND RAILWAY COMPANY LTD.

EAST-GRID
MT. TYNDALL AREA
WEST COAST TASMANIA

GRADIENT ARRAY DETAIL
DATA PROFILES

324077

5 cm

SURVEYED AND COMPILED BY
SCINTREX PTY. LTD.

DECEMBER 1973

200 0 200 400 feet
Scale 1:2400

JOB No. TAS. 018 C SHEET 1 of 1 PLATE 5

84-2236 vol 2
047

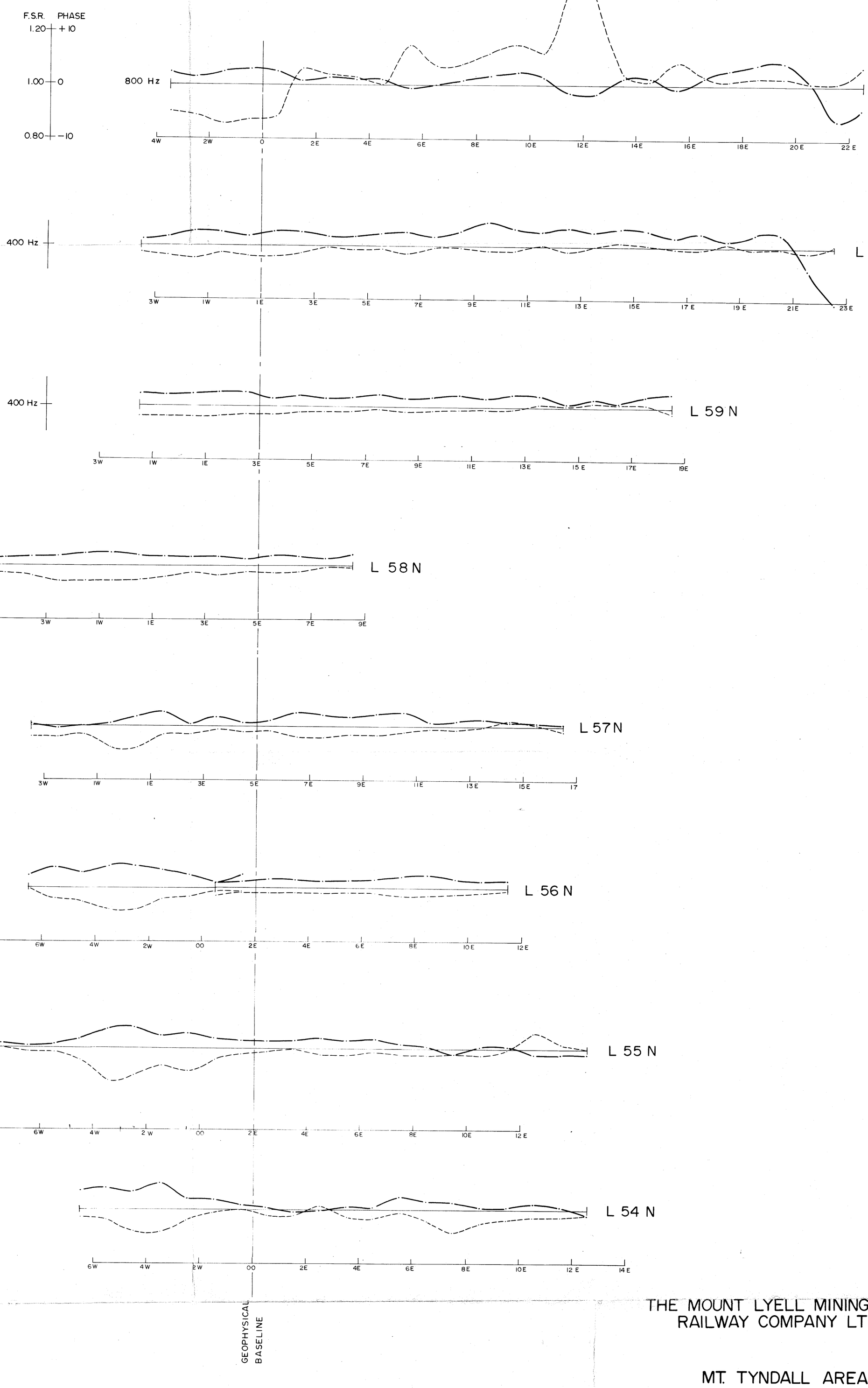

LEGEND

F. S.R. FREQUENCY PHASE
400 & 800 Hz.
F.S.R. PHASE
1.20 + 10°
1.00 0 Base Level
0.80 − 10°

THE MOUNT LYELL MINING AND RAILWAY COMPANY LTD.

MT. TYNDALL AREA
WEST COAST TASMANIA

TURAM ELECTROMAGNETIC SURVEY
DATA PROFILES

324078

5 cm

SURVEYED AND COMPILED BY
SCINTREX PTY. LTD.

DECEMBER 1973

200 0 200 400 feet
Scale 1:2400

JOB No. TAS.018 C SHEET 1 of 1

25(c)
000

324079

OPEN FILE

REPORT ON
DETAILED ELECTRICAL GEOPHYSICAL SURVEYS
MT. TYNDALL AREA, NEAR QUEENSTOWN, TASMANIA
ON BEHALF OF
THE MOUNT LYELL MINING AND RAILWAY COMPANY LTD.

TABLE OF MEASUREMENTS

001

324080

(PLATE 1)

5FT. THREE ARRAY LOG

DDH HFZ1, LINE 63

RESISTIVITY IN OHM-METRES

CHARGEABILITY IN MILLISECONDS

DEPTH IN FEET

Depth	Resistivity	Chargeability	L/M
40'	440	2.3	2.09
45'	345	0.75	4.67
50'	306	-1.5	-1.87
55'	297	-1.9	-1.21
60'	249	-2.8	-0.64
65'	213	-7.0	-0.04
70'	266	-7.0	-0.04
75'	172	-7.4	-0.03
80'	383	-3.3	-0.61
85'	451	-6.0	0.04
90'	551	-4.5	-0.11
95'	599	-4.9	-0.10
100'	718	-5.0	-0.15
105'	775	-1.5	-1.87
110'	517	-3.8	-0.34
115'	551	-6.3	0.04
120'	420	-7.4	0.07
125'	394	-5.8	-0.04
130'	410	-0.5	-7.00
135'	322	-1.0	-3.30
140'	383	0.25	16.00
145'	410	2.8	2.07
150'	440	8.8	1.00
155'	599	8.8	1.08
160'	649	-0.5	-6.6
165'	597	-2.8	-0.64

Depth	Resistivity	Chargeability	L/M
170'	649	-5.0	-0.05
175'	620	-3.8	-0.26
180'	517	-3.5	-0.37
185'	499	1.3	3.31
190'	587	1.9	2.11
195'	597	6.5	1.12
200'	528	2.8	1.96
205'	323	-2.6	-0.96
210'	400	1.6	1.44
215'	296	-2.6	0.77
220'	379	-1.5	-1.67
225'	441	-6.5	0.15
230'	505	-6.3	0.16
235'	603	-3.5	-0.29
240'	597	-2.5	-0.92
245'	597	7.0	1.14
250'	413	13.0	0.88
255'	441	14.0	0.91
260'	471	24.0	0.79
265'	1021	-2.8	-0.82
270'	919	8.0	1.06
275'	1165	30.0	0.73
280'	130	42.4	0.92
285'	342	12.0	1.11
290'	976	16.5	0.84
295'	364	25.0	0.67

Depth	Resistivity	Chargeability	L/M
300'	751	16.6	0.84
305'	574	17.5	0.86
310'	492	19.0	0.87
315'	198	52.1	0.66
320'	63.8	48.4	0.77
325'	27.75	99.0	0.82
330'	106	64.5	0.77
335'	120	37.9	0.87
340'	233	33.0	0.82
345'	496	11.0	1.00
350'	459	14.8	0.98
355'	242	36.0	0.79
360'	205	36.8	0.82
365'	679	11.5	1.04
370'	833	10.25	1.10
375'	689	3.3	2.12
380'	774	4.3	1.86
385'	651	7.3	1.30
390'	994	16.5	1.02
395'	1302	10.3	1.15
400'	320	47.3	0.68
405'	163	82.1	0.64
410'	746	88.0	0.65
415'	574	68.6	0.61
420'	332	54.8	0.66
425'	287	74.3	0.58

Depth	Resistivity	Chargeability	L/M
430'	250	60.8	0.64
435'	880	28.0	0.77
440'	637	17.0	0.85
445'	804	11.1	0.99
450'	1212	12.8	1.00
455'	492	21.1	0.88
460'	195	47.3	0.67
465'	359	45.0	0.72
470'	557	59.3	0.67
475'	1019	5.8	1.55
480'	783	10.8	1.16
485'	597	2.8	2.50
490'	731	2.5	2.40
495'	459	8.0	1.25
500'	488	12.8	0.78
505'	488	-3.3	0.45
510'	271	-7.6	-0.03
515'	328	-12.0	0.21

006

324085

(PLATE 2)

SCHLUMBERGER ELECTRICAL SOUNDING

LINE 56 AT 00

'a' IN FEET

'b' IN FEET

RESISTIVITY IN OHM-METRES

CHARGEABILITY IN MILLIVOLTS/VOLT

'a'	'b'	Resistivity	Chargeability M_1	M_3	M_5
10	3	4743	7.2	7	6.8
20	3	3080	7.8	7.4	7.2
40	3	1979	11	9.5	8.7
60	3	1035	4.1	2.7	3.1
60	5	1119	10.3	10.5	9.6
100	3	510	10.5	11.3	10.2
100	5	637	12.7	13.4	12.3
150	5	465	13.8	13.5	13.5
150	10	363	14.6	14.1	14.0
150	25	387	13.9	13.4	13.0
200	10	323	11.0	11.0	10.5
200	25	390	14.1	14.1	13.9
400	10	613	12.7	12.6	12.6
400	25	615	12.1	12.1	12.1
750	25	1623	10.7	10.7	10.8
750	50	1663	9.5	9.5	9.4
1000	25	2353	10.1	10.0	10.0
1000	50	2177	9.5	9.1	9.1

(PLATE 3)

CLOSE COUPLED ARRAY DETAIL

POLE-DIPOLE

RESISTIVITY IN OHM-METRES

CHARGEABILITY IN MILLIVOLTS/VOLT

STATION INTERVAL IN FEET

Station	'n'	Resistivity	Chargeability M_1	M_3	M_5
Line 52N					
1.0E	1	638	10.4	10.0	9.8
2.0E	2	997	10.3	10.1	9.8
3.0E	1	773	11.1	11.4	11.4
4.0E	2	822	9.1	8.9	9.0
5.0E	1	950	7.2	6.8	6.8
6.0E	2	1281	6.8	6.2	6.7
7.0E	1	852	7.2	7.0	7.1
8.0E	2	1537	8.5	8.2	8.4
9.0E	1	777	8.5	8.2	8.3
10.0E	2	1336	9.0	8.7	8.7
11.0E	11	1473	9.9	9.4	9.4
12.0E	2	1424	8.0	7.6	7.6
13.0E	1	1698	10.8	10.6	10.8
14.0E	2	2331	9.8	9.5	9.7
15.0E	1	1800	10.3	9.7	9.7
16.0E	2	1231	9.9	9.6	9.6
17.0E	1	3095	15.5	14.5	14.5
18.0E	2	3796	12.8	12.2	12.3
19.0E	1	3551	18.0	16.5	16.3
20.0E	2	2766	13.5	12.5	12.3
21.0E	1	2429	12.4	11.5	11.5
22.0E	2	3233	10.8	10.0	10.1
23.0E	1	4478	16.9	15.4	15.6

Station	'n'	Resistivity	Chargeability M_1	M_3	M_5
24.0E	2	6202	13.3	12.6	12.6
25.0E	1	4596	11.7	10.7	10.7
26.0E	2	3776	11.5	10.7	10.7
27.0E	1	9880	14.8	13.6	13.5
Line 53N					
1.0E	1	1580	8.5	8.0	8.0
3.0E	1	1515	8.4	8.4	8.4
4.0E	2	2222	7.5	7.1	7.1
5.0E	1	1341	9.0	8.2	8.1
6.0E	2	1952	9.1	8.5	8.4
7.0E	1	546	11.3	10.5	10.5
8.0E	2	1455	10.8	10.1	10.1
9.0E	1	1932	9.3	8.8	8.8
10.0E	2	1737	8.7	8.4	8.5
11.0E	1	1547	7.2	6.6	6.7
12.0E	2	1165	6.3	6.0	6.0
13.0E	1	1149	3.1	2.8	2.8
14.0E	2	2122	4.5	4.2	4.2
15.0E	1	1356	6.2	5.8	5.8
16.0E	2	2395	6.7	6.3	6.3
17.0E	1	1398	6.3	6.0	6.0
18.0E	2	1861	5.8	5.6	5.6
19.0E	1	1436	9.7	9.3	9.4

Station	'n'	Resistivity	Chargeability		
			M_1	M_3	M_5
20.0E	2	2067	9.1	8.8	8.8
21.0E	1	3179	9.4	9.0	9.0
22.0E	2	5245	9.3	8.9	8.9
23.0E	1	3830	10.4	10.1	10.1
24.0E	2	4824	11.0	10.5	10.5
25.0E	1	4596	11.2	10.6	10.6
26.0E	2	6968	11.7	11.1	11.2
27.0E	1	4507	11.5	10.6	10.6
27.5E	1.5	5407	11.4	10.6	10.6
28.5E	0.5	3474	13.1	12.0	11.8

012

324091

(PLATE 3)

CLOSE COUPLED ARRAY DETAIL

THREE-ARRAY

RESISTIVITY IN OHM-METRES

CHARGEABILITY IN MILLIVOLTS/VOLT

STATION INTERVAL IN FEET

Station	'a'	Resistivity	Chargeability M_1	M_3	M_5
Line 52N					
1.5E	100'	533	8.4	8.2	8.2
2.5E	100'	648	9.8	9.5	9.5
2.75E	50'	383	9.5	9.1	9.1
3.25E	50'	1395	9.4	9.0	9.0
3.5E	100'	1259	9.0	8.7	8.7
3.75E	50'	2598	12.8	12.2	12.2
4.25E	50'	1333	17.3	16.5	16.5
4.5E	100'	1077	11.8	11.5	11.5
4.75E	50'	1866	16.8	16.1	16.1
5.25E	50'	718	11.2	10.8	10.8
5.5E	100'	621	8.2	7.7	7.7
5.75E	50'	354	10.2	9.6	9.6
6.25E	50'	689	14.0	13.1	13.1
6.5E	100'	757	10.2	9.6	9.6
6.75E	50'	798	19.3	18.0	18.0
7.25E	50'	912	21.0	20.0	20.0
7.5E	100'	236	8.3	7.8	7.7
7.75E	50'	200	9.7	9.0	9.0
8.25E	50'	269	4.8	4.5	4.5
		*******			
19.5E	100'	3375	18.3	16.9	16.8
19.75E	50'	1708	12.5	11.7	11.7
20.0E	100'	3634	15.9	14.8	14.8

Station	'a'	Resistivity	Chargeability M_1	M_3	M_5
20.25E	50'	1715	15.4	13.8	13.1
20.5E	100'	3309	15.5	14.3	14.2
20.75E	50'	2381	17.5	16.2	16.0
21.0E	100'	4294	16.7	15.7	15.7
21.25E	50'	1579	20.5	18.8	18.7
21.5E	100'	3283	16.2	15.0	14.8
21.75E	50'	1796	19.1	17.8	17.8
22.0E	100'	2729	17.4	16.3	16.3
22.25E	50'	1364	17.9	16.4	16.3
22.5E	100'	4005	18.4	17.3	17.3
22.75E	50'	2018	14.2	12.9	12.9
22.75E	100'	3359	15.9	14.8	15.0
23.0E	50'	2029	11.0	9.8	9.6
23.25E	100'	2488	12.0	11.0	11.0
23.5E	50'	1445	12.8	12.0	12.2
23.75E	100'	2752	10.9	10.2	10.2
24.0E	50'	2354	10.6	9.7	9.7
24.5E	100'	2930	11.1	10.1	10.0
24.75E	50'	1790	12.2	11.3	11.3
25.0E	100'	3543	12.1	11.3	11.1
25.25E	50'	1770	11.5	10.2	10.0
25.5E	100'	4153	13.8	12.7	12.6
25.75E	50'	3582	12.3	11.1	11.0
26.0E	100'	5903	13.3	12.3	12.2
26.25E	50'	4278	13.7	12.5	12.4
26.5E	100'	7756	14.5	13.3	13.1

Station	'a'	Resistivity	Chargeability M_1	M_2	M_5
26.75E	50'	5431	15.4	14,2	14.1
27.0E	100'	10232	16.0	14.7	14.5
27.25E	50'	7984	16.2	14.8	14.5
27.5E	100'	14707	17.0	15.5	15.4
Line 53N					
0.25E	50'	1148	9.8	9.2	9.2
0.50E	100'	1666	7.4	6.8	6.8
0.75E	50'	1179	8.6	8.0	8.0
1.0E	100'	1330	7.8	7.4	7.4
1.25E	50'	746	7.8	7.4	7.4
1.5E	100'	1509	8.2	7.6	7.6
1.75E	50'	772	7.8	7.3	7.3
2.0E	100'	1372	8.2	7.6	7.6
2.25E	50'	995	8.7	8.1	8.1
2.5E	100'	1806	8.5	8.0	8.0
2.75E	50'	1794	9.2	8.6	8.6
3.0E	100'	2183	8.3	7.7	7.7
3.25E	50'	1270	8.7	8.1	8.1
3.5E	100'	1005	8.6	8.0	8.0
3.75E	50'	702	9.2	8.6	8.6
4.0E	100'	757	9.2	8.5	8.5
4.25E	50'	616	9.9	9.3	9.2
4.5E	100'	530	10.8	10.0	9.9
4.75E	50'	354	10.9	10.3	10.3
5.0E	100'	527	11.3	10.5	10.5

Station	'a'	Resistivity	Chargeability M_1	M_2	M_3
5.25E	50'	292	12.3	11.6	11.6
5.5E	100'	622	9.4	8.7	8.7
5.75E	50'	166	12.2	11.4	11.4
6.0E	100'	814	8.2	7.6	7.6
6.25E	50'	450	9.8	9.2	9.3
		*******			
22.5E	100'	2853	9.6	8.6	8.4
22.75E	50'	2517	9.8	8.4	8.0
23.0E	100'	3004	9.9	9.2	9.1
23.25E	50'	4402	14.7	13.3	13.1
23.5E	100'	2840	10.6	10.0	10.0
23.75E	50'	3281	14.0	12.7	12.5
24.0E	100'	3016	11.0	10.0	9.8
24.25E	50'	3062	10.6	9.0	8.7
24.5E	100'	3119	10.3	9.6	9.5
24.75E	50'	2609	9.6	8.6	8.3
25.0E	100'	3217	9.7	9.0	8.9
25.25E	50'	2259	10.4	9.6	9.5
25.5E	100'	2260	9.5	8.6	8.5
25.75E	50'	2488	14.0	13.2	13.0
26.0E	100'	2298	9.6	8.8	8.7
26.25E	50'	1501	10.5	9.4	9.3
26.5E	100'	2355	10.6	9.9	9.7
26.75E	50'	1802	11.4	10.4	10.3
27.0E	100'	2528	10.6	9.5	9.3

Station	'a'	Resistivity	Chargeability M_1	M_3	M_5
27.25E	50'	1302	9.8	8.8	8.5
27.5E	100'	2624	11.2	10.2	10.2
27.75E	50'	1904	11.5	10.2	9.8
28.0E	100'	3217	12.4	11.2	11.0
28.25E	50'	1837	11.0	9.8	9.7
28.5E	100'	3485	12.8	11.8	11.8
28.75E	50'	2775	10.1	9.1	8.9

(PLATE 4)

GRADIENT ARRAY DETAIL

WEST GRID

RESISTIVITY IN OHM-METRES

CHARGEABILITY IN MILLISECONDS

STATION INTERVAL IN FEET

Station	Resistivity	Chargeability	L/M
Current Electrodes at 20W and 30E on Line 26			
Line 28			
17.5W	763	65.0	-
16.5W	6582	1.8	0.56
15.5W	2676	-13.9	0.99
14.5W	2837	10.6	0.83
13.5W	3754	24.8	0.77
12.5W	12194	24.6	0.80
11.5W	20088	21.5	0.79
10.5W	8932	22.0	0.82
9.5W	5966	24.1	0.79
8.5W	4948	30.0	0.75
7.5W	3785	34.3	0.81
6.5W	3607	19.0	0.79
5.5W	3559	27.5	0.80
4.5W	3195	28.5	0.84
3.5W	5106	28.5	0.79
2.5W	3948	31.0	0.77
1.5W	3878	31.5	0.79
0.5W	2870	30.0	0.85
0.5E	1873	29.8	0.87
1.5E	1295	32.3	0.81
2.5E	1455	30.0	0.81
3.5E	1157	29.3	0.62
4.5E	2367	29.0	0.78
5.5E	2659	29.4	0.78

Station	Resistivity	Chargeability	L/M
6.5E	3338	24.0	0.87
7.5E	1775	27.4	0.93
8.5E	1265	34.0	0.66
9.5E	1580	25.3	0.86
10.5E	1034	36.0	0.79
11.5E	1104	36.0	0.80
12.5E	2160	39.0	0.77
13.5E	2636	34.0	0.85
14.5E	2791	33.0	0.95
15.5E	2355	32.0	0.94
16.5E	1484	31.5	0.89
17.5E	1624	22.3	0.92
18.5E	1127	18.5	0.78
19.5E	374	12.5	0.94
20.5E	232	-	-
Current Electrodes at 18.5W and 1.5E on Line 26			
Line 26			
17.5W	4430	18.3	0.83
16.5W	2160	17.0	0.79
15.5W	4120	19.0	0.72
14.5W	5530	16.9	0.69
13.5W	4856	16.9	0.76
12.5W	1965	20.0	0.75
11.5W	2063	22.0	0.75
10.5W	2535	18.3	0.75
9.5W	1805	21.8	0.68
9.0W	1515	26.3	0.66

Station	Resistivity	Chargeability	L/M
8.5W	974	27.0	0.72
8.5W	974	27.0	0.74
8.0W	696	36.0	0.61
7.5W	916	35.5	0.68
6.5W	900	27.8	0.79
5.5W	423	22.3	0.73
Current Electrodes at 20W and 30E on Line 26			
Line 26			
6.5W	5071	36.5	0.84
5.5W	6192	27.5	0.85
4.5W	2914	34.4	0.78
3.5W	4555	29.4	0.83
2.5W	3766	26.0	0.81
1.5W	2070	31.3	0.74
0.5W	1168	28.0	0.89
0.5E	925	33.0	0.68
1.5E	1225	29.3	0.66
2.5E	1262	28.0	0.75
3.5E	3233	27.8	0.67
4.5E	1018	36.5	0.64
5.5E	1475	36.8	0.66
6.5E	438	48.0	0.65
7.5E	440	45.5	0.66
8.5E	467	39.5	0.65
9.5E	924	33.0	0.63
10.5E	1699	20.5	0.79
11.5E	888	19.3	0.72
12.5E	1014	18.8	0.76

Station	Resistivity	Chargeability	L/M
13.5E	591	17.5	0.74
14.5E	786	24.0	0.66
15.5E	870	27.3	0.69
16.5E	900	29.5	0.71
17.5E	709	28.8	0.67
18.5E	532	23.9	0.70
19.5E	121	25.8	0.67
20.5E	441	29.3	0.65
21.5E	745	23.4	0.71
Line 24			
16.5W	15628	12.8	0.66
15.5W	10180	15.0	0.77
15.0W	9192	19.0	0.74
14.5W	9015	20.2	0.76
14.0W	14278	18.0	0.69
13.5W	14406	14.0	0.70
12.5W	3944	12.5	0.80
12.0W	3301	21.0	0.71
11.5W	7641	27.7	0.65
10.5W	6559	27.7	0.71
9.5W	4551	29.2	0.62
9.0W	3831	28.0	0.55
8.5W	3242	18.7	0.76
8.0W	2360	22.5	0.71
7.5W	7048	30.0	0.73
6.5W	4956	27.7	0.70
5.5W	3893	32.0	0.66
4.5W	1894	30.7	0.66
3.5W	2045	30.0	0.68
2.5W	1912	28.5	0.76
1.5W	2137	28.5	0.76

Station	Resistivity	Chargeability	L/M
0.5W	1085	30.0	0.75
0.5E	955	31.5	0.63
1.0E	1201	40.7	0.59
1.5E	1480	39.0	0.72
2.0E	1462	33.0	0.64
2.5E	1194	33.0	0.64
3.0E	1260	35.0	0.64
3.5W	1165	37.5	0.62
4.0E	953	45.0	0.60
4.5E	902	40.0	0.60
5.5E	1116	34.5	0.61
6.5E	1290	25.5	0.50
7.5E	1320	21.2	0.47
8.5E	1138	25.5	0.51
9.5E	2864	18.0	0.66
10.5E	2784	20.5	0.55
11.5E	1900	22.4	0.59
12.5E	1822	25.0	0.64
13.5E	2573	28.0	0.75
14.5E	3360	25.5	0.78
15.5E	3656	12.5	0.88
16.5E	5024	10.0	0.70
17.5E	-	9.0	0.89
18.5E	-	9.0	0.78
19.5E	-	8.0	1.00

024

324103

(PLATE 5)

GRADIENT ARRAY DETAIL

EAST GRID

RESISTIVITY IN OHM-METRES

CHARGEABILITY IN MILLISECONDS

STATION INTERVAL IN FEET

Station	Resistivity	Chargeability	L/M
ZONE 'A'			
Current Electrodes at 10W and 10E on line 6			
Line 6 + 400N			
4.5W	615	10.0	0.98
3.5W	1765	9.5	0.95
2.5W	2400	15.3	0.85
1.5W	2850	26.3	0.75
0.5W	2240	28.8	0.81
0.5E	2085	31.5	0.81
1.5E	1525	31.5	0.81
2.5E	1120	33.0	0.80
3.5E	1295	31.5	0.76
4.5E	1800	29.8	0.72
5.5E	2160	17.5	0.70
6.5E	4720	12.8	0.81
7.5E	4720	9.0	0.78
Line 6 + 00			
6.5W	1710	14.1	0.91
5.5W	3030	12.3	0.94
4.5W	3115	19.5	0.88
3.5W	2065	23.2	0.91
2.5W	3290	29.3	0.82
2.0W	4500	36.4	0.78
1.5W	3860	41.2	0.78
1.0W	1525	35.6	0.89
0.5W	1055	36.7	0.82
00	1480	41.3	0.85
0.5E	1463	49.7	0.77
1.25E	925	42.0	0.80

Station	Resistivity	Chargeability	L/M
1.5E	920	40.5	0.84
1.75E	1220	40.7	0.77
2.5E	1735	37.2	0.75
3.5E	1900	33.0	0.82
4.5E	3450	26.2	0.86
5.5E	4100	7.5	1.07
Line 6 + 400S			
0.5E	2400	7.3	0.93
1.5E	2420	11.0	0.82
2.5E	2780	14.9	0.87
3.0E	1675	25.1	0.85
3.5E	2210	26.6	0.80
4.0E	1440	20.3	0.94
4.5E	1510	19.9	0.82
5.0E	1160	26.3	0.86
5.5E	1755	33.8	0.84
6.0E	1470	39.0	0.81
6.5E	1860	35.6	0.78
7.0E	1450	33.8	0.80
7.5E	1680	33.0	0.82
8.5E	1210	29.8	0.76
9.5E	1445	30.0	0.80
ZONE 'B'			
Current Electrodes at 46E and 66E on Line 4			
Line 4			
49.5E	770	7.1	0.96
50.5E	2300	5.3	0.94
51.5E	1840	14.6	0.84
52.0E	1835	20.8	0.74
52.5E	1160	25.8	0.83
53.0E	1125	27.8	0.79
53.5E	1165	22.5	0.82
54.5E	960	21.8	0.77

Station	Resistivity	Chargeability	L/M
55.5E	2210	21.8	0.79
56.0E	2870	21.6	0.76
56.5E	3150	21.9	0.71
57.0E	2390	22.4	0.69
57.5E	2230	20.5	0.75
58.5E	1065	9.9	0.81
59.5E	655	6.5	0.82
60.5E	464	6.0	0.88
ZONE 'C3'			
Current Electrodes at 32W and 12W on Line 22 + 00			
Line 22 + 200N			
26.5W	735	14.1	0.78
25.5W	908	17.3	0.78
24.5W	1355	19.0	0.74
23.5W	2150	18.8	0.77
22.5W	2250	18.3	0.75
21.5W	1790	19.1	0.77
20.5W	2690	20.4	0.81
19.5W	3230	14.5	0.78
18.5W	4140	11.5	0.77
17.5W	2230	13.0	0.69
Line 22 + 00			
26.5W	1000	13.3	0.83
25.5W	1080	12.6	0.79
24.5W	602	11.6	0.85
23.5W	1070	19.8	0.76
22.5W	2270	22.0	0.76

Station	Resistivity	Chargeability	L/M
21.5W	1985	22.3	0.74
20.5W	1940	16.5	0.79
20.0W	1840	18.3	0.78
19.5W	1213	29.3	0.80
19.0W	1195	25.5	0.75
18.5W	980	20.3	0.76
17.5W	1950	13.8	0.94
16.5W	2560	12.1	0.83
Line 22 + 200S			
25.5W	532	11.1	0.97
24.5W	765	14.0	1.00
24.0W	923	20.6	0.91
23.5W	932	26.6	0.85
22.5W	1295	30.0	0.80
21.5W	3000	20.3	0.83
20.5W	1360	24.5	1.01
20.0W	1235	28.8	0.91
19.5W	1000	24.0	0.97
18.5W	550	27.4	0.91
18.0W	898	23.6	0.90
17.5W	802	-77.2	0.68
17.0W	3080	15.8	0.92
ZONE 'C4'			
Current Electrodes at 10E and 50W on Line 40N			
Line 40N			
46.5W	3740	16.3	0.74
45.5W	2960	19.8	0.65
44.5W	4540	27.8	0.67
43.5W	4420	18.8	0.76
42.5W	3550	17.0	0.74

Station	Resistivity	Chargeability	L/M
41.5W	3770	18.3	0.73
40.5W	5230	17.5	0.71
39.5W	5190	13.1	0.67
38.5W	6570	12.3	0.71
37.5W	5410	11.3	0.93
36.5W	6260	10.5	0.93
36.0W	4410	11.9	0.86
35.5W	3000	15.0	0.83
34.5W	3460	14.3	0.76
33.5W	6840	8.9	0.82
32.5W	8350	10.3	0.88
31.5W	9900	9.9	0.89
30.5W	17570	11.3	0.80
29.5W	7720	10.4	0.82
28.5W	16250	10.4	0.82
27.5W	5860	11.0	0.75
26.5W	6880	12.1	0.72
25.5W	6580	13.9	0.77
24.5W	2170	14.5	0.72
23.5W	5750	10.9	0.80
22.5W	9250	9.0	0.78
21.5W	7460	7.8	0.77
20.5W	6200	8.0	0.84
19.5W	6630	9.3	0.89
18.5W	5540	9.8	0.85
17.5W	6310	10.3	0.78
16.5W	9850	10.1	0.84

Station	Resistivity	Chargeability	L/M
15.5W	7500	13.3	0.71
14.5W	8700	11.6	0.82
13.5W	5400	10.8	0.97
12.5W	10100	11.4	0.75
11.5W	5210	12.5	0.78
10.5W	2990	11.6	0.82
9.5W	2730	16.1	0.80
8.5W	3800	19.1	0.73
8.5W	3520	18.8	0.68
7.5W	3480	29.5	0.67
7.0W	3090	34.7	0.66
6.5W	2740	34.0	0.66
6.0W	4280	21.0	0.70
5.5W	3560	17.3	0.71
5.0W	1640	19.1	0.76
4.5W	2460	19.0	0.67
4.0W	3160	17.4	0.59
3.5W	4010	7.6	0.96
2.5W	8800	6.5	0.82
1.5W	5970	7.0	0.72
0.5W	3010	7.8	0.77
Line 38N			
47.5W	4570	22.9	0.72
46.5W	5410	28.8	0.69
45.5W	6460	28.5	0.73
44.5W	7280	30.0	0.71
43.5W	5970	26.8	0.75
42.5W	7220	27.3	0.75
41.5W	4900	23.5	0.76

Station	Resistivity	Chargeability	L/M
40.5W	4120	25.4	0.83
40.0W	1462	32.3	0.81
39.5W	3750	21.9	0.89
39.0W	3697	11.5	0.87
38.5W	11300	1.8	1.67
37.5W	13850	1.5	1.50
36.5W	21300	4.0	1.07
35.5W	18850	4.8	1.10
34.5W	12500	8.3	1.00
34.0W	8304	13.8	0.87
33.5W	5650	34.3	0.79
32.5W	7950	21.0	0.83
32.0W	7790	20.0	0.92
31.5W	13700	15.3	0.87
31.0W	12805	9.0	0.98
30.5W	14500	6.0	1.00
29.5W	15700	8.0	0.94
28.5W	22100	7.5	0.97
27.5W	13900	6.8	1.07
26.5W	12600	6.8	1.00
25.5W	11600	8.8	1.00
24.5W	17700	8.0	0.79
23.5W	9800	10.8	0.82
22.5W	12850	11.3	0.79
21.5W	9300	8.8	1.00
20.5W	9400	10.4	0.91
19.5W	7450	11.8	0.96
19.0W	5890	14.0	0.86
18.5W	5330	14.1	0.91
17.5W	6120	9.3	1.07
16.5W	5940	9.3	1.05
15.5W	4120	10.0	0.88

Station	Resistivity	Chargeability	L/M
14.5W	4480	9.5	1.00
13.5W	4300	16.1	1.01
12.5W	4800	28.5	0.77
11.5W	3550	23.8	0.84
11.0W	2091	27.4	0.77
10.5W	2900	39.0	0.85
9.5W	5104	14.6	0.91
8.5W	8525	9.9	1.01
7.5W	10592	9.1	0.99
6.5W	7429	9.8	0.87
5.5W	7791	9.3	0.86
4.5W	6605	10.9	0.85
3.5W	3994	12.6	0.90
2.5W	5678	12.0	0.90
1.5W	7568	12.0	0.90
0.5W	4171	10.4	1.01
Current Electrodes at 9W and 29W on Line 34N			
Line 34N			
25.5W	894	12.5	0.80
24.5W	905	12.1	0.77
23.5W	1224	12.0	0.73
22.5W	1633	11.5	0.72
21.5W	2022	11.3	0.71
20.5W	987	10.3	0.85
19.5W	385	9.4	0.85
18.5W	568	13.3	0.75
17.5W	970	11.0	0.82

Station	Resistivity	Chargeability	L/M
16.5W	2811	9.5	0.79
15.5W	4408	8.3	0.78
Current Electrodes at 40W and 20W on Line 28N			
Line 28N			
33.5W	7680	10.3	0.92
32.5W	4600	9.8	0.97
31.5W	3270	11.3	0.89
30.5W	1395	9.0	0.92
29.5W	473	5.6	0.98
28.5W	476	2.8	1.00
27.5W	1200	7.3	0.79
26.5W	1415	8.3	0.78
25.5W	1255	9.3	0.75
24.5W	1380	9.0	0.81
23.5W	970	9.0	0.76

034

324113

(PLATE 6)

TURAM ELECTROMAGNETICS

Station	Phase	Field Strength Ratio
400Hz		
Line 61N		
3.5W	- 5.0	1.05
2.5W	- 5.5	1.03
1.5W	- 7.0	1.05
0.5W	- 6.5	1.06
0.5E	- 6.0	1.05
1.5E	+ 3.0	1.02
2.5E	+ 2.0	1.03
3.5E	+ 1.5	1.02
4.5E	0	1.02
5.5E	+ 7.5	0.99
6.5E	+ 3.5	1.00
7.5E	+ 4.0	1.02
8.5E	+ 6.0	1.04
9.5E	+ 7.5	1.05
10.5E	+ 6.0	1.03
11.5E	+19.0	0.97
12.5E	+20.0	0.97
13.5E	+ 2.0	1.03
14.5E	+ 1.0	1.03
15.5E	+ 4.5	0.99
16.5E	+ 2.0	1.03
17.5E	+ 1.0	1.06
18.5E	+ 1.5	1.08

Station	Phase	Field Strength Ratio
19.5E	+ 1.5	1.09
20.5E	+ 0.5	1.02
800Hz		
Line 61N		
3.5W	-20.0	1.09
2.5W	-17.0	1.06
1.5W	-14.0	1.03
0.5W	-11.0	1.07
0.5E	- 7.0	1.04
1.5E	+ 6.0	1.01
2.5E	+ 6.0	1.01
3.5E	+ 3.5	0.99
4.5E	+ 1.5	1.03
5.5E	+12.0	0.94
6.5E	+ 7.0	0.99
7.5E	+ 8.5	1.01
8.5E	+12.0	1.02
9.5E	+16.0	1.07
10.5E	+ 9.5	1.04
11.5E	+15.0	1.03
12.5E	+14.0	1.18
13.5E	+ 5.0	1.05
14.5E	+ 2.5	1.02

Station	Phase	Field Strength Ratio
15.5E	+ 2.5	1.04
16.5E	+ 2.0	1.05
17.5E	+ 1.0	1.05
18.5E	+ 1.5	1.08
19.5E	+ 1.5	1.08
20.5E	+ 1.5	1.10
21.5E	+ 0.5	1.15
22.5E	+ 3.0	1.20

Station	Phase	Field Strength Ratio
800Hz		
Line 61N		
6.5E	+ 3.0	1.02
7.5E	+ 6.0	1.00
8.5E	+10.0	1.00
9.5E	+ 6.0	1.04
10.5E	+ 7.0	1.01
11.5E	+11.0	0.99
12.5E	+ 6.5	1.04
13.5E	+ 1.5	1.05
14.5E	+ 0.5	1.04
400Hz		
Line 60N		
3.5W	- 1.5	1.025
2.5W	- 2.0	1.033
1.5W	- 2.5	1.054
0.5W	- 1.5	1.047
0.5E	- 2.0	1.035
1.5E	- 2.0	1.052
2.5E	- 1.5	1.049
3.5E	- 0.5	1.036
4.5E	- 1.0	1.037
5.5E	- 0.5	1.043
6.5E	- 1.5	1.052
7.5E	- 0.5	1.038
8.5E	- 0.5	1.056

Station	Phase	Field Strength Ratio
9.5E	- 1.0	1.090
10.5E	- 1.0	1.065
11.5E	0	1.057
12.5E	- 1.0	1.066
13.5E	0	1.054
14.5E	+ 0.5	1.062
15.5E	0	1.058
16.5E	- 0.5	1.035
17.5E	- 0.5	1.051
18.5E	+ 0.5	1.022
19.5E	- 0.5	1.047
20.5E	- 0.5	1.045
21.5E	- 1.0	0.916
22.5E	0	0.781
400Hz		
Line 59N		
1.5W	- 2.0	1.041
0.5W	- 2.0	1.042
0.5E	- 2.0	1.041
1.5E	- 2.0	1.047
2.5E	- 1.5	1.057
3.5E	- 1.5	1.026
4.5E	- 1.0	1.041
5.5E	- 1.0	1.033
6.5E	- 1.0	1.033
7.5E	- 0.5	1.041

Station	Phase	Field Strength Ratio
8.5E	- 1.0	1.028
9.5E	- 1.0	1.035
10.5E	- 0.5	1.041
11.5E	- 0.5	1.033
12.5E	- 0.5	1.043
13.5E	+ 0.5	1.040
14.5E	+ 0.5	1.015
15.5E	+ 1.0	1.026
16.5E	+ 1.0	1.013
17.5E	+ 0.5	1.039
18.5E	- 1.0	1.047
Line 58N		
5.5W	- 1.5	1.022
4.5W	- 1.5	1.030
3.5W	- 2.0	1.033
2.5W	- 3.0	1.035
1.5W	- 3.0	1.043
0.5W	- 3.0	1.045
0.5E	- 3.0	1.039
1.5E	- 2.5	1.036
2.5E	- 1.5	1.033
3.5E	- 2.0	1.035
4.5E	- 1.5	1.023
5.5E	- 1.75	1.038
6.5E	- 1.5	1.034
7.5E	- 0.5	1.022

Station	Phase	Field Strength Ratio
8.5E	- 0.5	1.040
Line 57N		
3.5W	- 2.0	1.007
2.5W	- 2.0	0.996
1.5W	- 1.5	0.999
0.5W	- 4.0	1.011
0.5E	- 4.0	1.036
1.5E	- 1.5	1.053
2.5E	- 1.5	1.008
3.5E	- 0.5	1.038
4.5E	- 1.0	1.016
5.5E	- 1.0	1.023
6.5E	- 2.0	1.047
7.5E	- 2.0	1.044
8.5E	- 1.5	1.035
9.5E	- 1.5	1.045
10.5E	- 1.0	1.049
11.5E	- 0.5	1.017
12.5E	- 0.5	1.020
13.5E	0	1.023
14.5E	+ 1.0	1.016
15.5E	+ 0.5	1.017
16.5E	- 1.0	1.007
Line 56N		
6.5W	0	1.011
5.5W	- 2.0	1.037

Station	Phase	Field Strength Ratio
4.5W	- 2.5	1.021
3.5W	- 4.0	1.037
2.5W	- 4.0	1.036
1.5W	- 2.0	1.02
0.5W	- 1.5	1.003
0.5E	- 0.5	0.973
0.5E	- 1.5	1.021
1.5E	- 0.5	0.998
1.5E	- 1.0	1.023
2.5E	- 1.0	1.033
3.5E	- 1.0	1.030
4.5E	- 1.0	1.026
5.5E	- 1.0	1.027
6.5E	- 1.0	1.032
7.5E	- 1.5	1.040
8.5E	- 1.5	1.045
9.5E	- 1.5	1.034
10.5E	- 1.0	1.027
11.5E	- 0.5	1.025
800Hz		
Line 55N		
8.5W	0	1.02
7.5W	0	1.02
6.5W	- 0.5	1.01
5.5W	- 0.5	1.02
4.5W	- 2.0	1.04
3.5W	- 6.0	1.07

Station	Phase	Field Strength Ratio
2.5W	- 5.0	1.08
1.5W	- 3.0	1.05
0.5W	- 4.0	1.06
0.5E	- 2.0	1.04
1.5E	- 1.0	1.03
2.5E	- 0.5	1.03
3.5E	0	1.03
4.5E	- 1.0	1.04
5.5E	- 1.0	1.03
6.5E	- 0.5	1.04
7.5E	- 1.0	1.02
8.5E	- 1.0	1.01
9.5E	- 1.0	0.98
10.5E	- 1.0	1.01
11.5E	0	1.01
12.5E	+ 3.0	0.98
13.5E	+ 1.0	0.98
14.5E	0	0.98
Line 54N		
6.5W	- 1.5	1.07
5.5W	- 2.0	1.08
4.5W	- 4.0	1.07
3.5W	- 4.0	1.10
2.5W	- 2.0	1.04
1.5W	- 0.5	1.04
0.5W	0	1.02

Station	Phase	Field Strength Ratio
0.5E	- 1.0	1.01
1.5E	- 1.0	0.99
2.5E	+ 0.5	1.00
3.5E	- 1.5	1.01
4.5E	- 1.5	1.01
5.5E	- 0.5	1.05
6.5E	- 2.0	1.03
7.5E	- 4.0	1.03
8.5E	- 2.5	1.01
9.5E	- 2.0	1.01
10.5E	- 1.5	1.02
11.5E	- 1.5	1.01
12.5E	- 1.0	0.98